Pharm Res (2014) 31:1689–1709
DOI 10.1007/s11095-013-1273-3

RESEARCH PAPER

Arachidonic Acid-Modified Lovastatin Discoidal Reconstituted High Density Lipoprotein Markedly Decreases the Drug Leakage during the Remodeling Behaviors Induced by Lecithin Cholesterol Acyltransferase

Hongliang He • Lisha Liu • Hui Bai • Ji Wang • Yan Zhang • Wenli Zhang • Mengyuan Zhang • Zimei Wu • Jianping Liu

Received: 26 July 2013 / Accepted: 19 December 2013 / Published online: 22 January 2014

ABSTRACT

Purpose Our previous studies indicated that drug leaked from discoidal reconstituted high density lipoprotein (d-rHDL) during the remodeling behaviors induced by lecithin cholesterol acyl transferase (LCAT) abundant in circulation, thus decreasing the drug amount delivered into the target. In this study, arachidonic acid (AA)-modified d-rHDL loaded with lovastatin (LT) were engineered as AA-LT-d-rHDL to explore whether AA modification could reduce the drug leakage during the remodeling behaviors induced by LCAT and further deliver more drug into target cells to improve efficacy.

Methods After successful preparation of AA-LT-d-rHDL with different AA modification amount, a series of *in vitro* remodeling behaviors were investigated. Furthermore, inhibition on macrophage-derived foam cell formation was chosen to evaluate drug efficacy of AA-LT-d-rHDL.

Results *In vitro* physicochemical characterizations studies showed that all LT-d-rHDL and AA-LT-d-rHDL preparations had nano-size, negative surface charge, high entrapment efficiency (EE) and comparable drug loading efficiency (DL). With increment of AA modification amount, AA-LT-d-rHDL manifested lower reactivity with LCAT, thus significantly reducing the undesired drug leakage during the remodeling behaviors induced by LCAT, eventually exerting stronger efficacy on inhibition of macrophage-derived foam cell formation.

Conclusion AA-LT-d-rHDL could decrease the drug leakage during the remodeling behaviors induced by LCAT and fulfill efficient drug delivery.

H. He • L. Liu • J. Wang • W. Zhang • M. Zhang • J. Liu (✉)
Department of Pharmaceutics, China Pharmaceutical University No.24 Tongjia Lane, Nanjing 210009, People's Republic of China
e-mail: jianpingliu1293@163.com

H. Bai • Y. Zhang
Atherosclerosis Research Centre
Laboratory of Molecular Intervention with Cardiovascular Diseases
Nanjing Medical University, No.118
Hanzhong Road, Nanjing 210029, People's Republic of China

Z. Wu
School of Pharmacy University of Auckland
Private Bag 92019 Auckland, New Zealand

KEY WORDS arachidonic acid · d-rHDL · drug leakage · LCAT · remodeling behaviors

ABBREVIATIONS

AA	arachidonic acid
AA-LT-d-rHDL	AA-modified rHDL loaded with lovastatin
apoAI	apolipoprotein AI
CE	cholesterol esters
d-HDL	discoidal HDL
d-rHDL	discoidal reconstituted HDL
DL	drug loading efficiency
EE	entrapment efficiency
FC	free cholesterol
HDL	high density lipoprotein
LCAT	lecithin cholesterol acyltransferase
LT	lovastatin
LT-d-rHDL	rHDL loaded with lovastatin
LT-L	lovastatin liposome
LT-S	lovastatin solution
MDF	maximum denaturation fluorescence
MTT	3-(4, 5-dimethylthiazol-2-yl)-2, 5-diphenyltetrazolium bromide
RC	reduced cholesterol
RCT	reverse cholesterol transport
rHDL	reconstituted HDL
s-HDL	spherical HDL
s-rHDL	spherical reconstituted HDL
TC	total cholesterol
TEM	transmission electron microscopy

INTRODUCTION

High density lipoprotein (HDL), one of the endogenous lipoproteins in blood, exists in two structural forms, the discoidal

and the spherical (seen in the Fig. 1). The discoidal HDL (d-HDL) mature into spherical HDL (s-HDL) catalyzed by LCAT in the circulation, which is often regarded as remodeling behaviors as well as the essential step of reverse cholesterol transport (RCT). Recently, an increasing number of researches have demonstrated that HDL exerts antiatherogenic efficacies ascribed to exclusive RCT, anti-inflammation, anti-oxidation as well as enhancement of the nitric oxide (NO) production, etc. Hence, HDL are always referred to as good cholesterol or healthy symbol of cardiovascular system (1).

Reconstituted high density lipoprotein (rHDL) has been extensively utilized as drug delivery vehicles for genes (2,3), antitumor drugs (4,5) and cardiovascular drugs (6,7) due to the mentioned above distinctive structures and bioactive attributes. Among them, we have successfully constructed two structural rHDL as carriers for Tanshinone IIA (TA), respectively, and thoroughly investigated their *in vitro* characterizations and *in vivo* antiatherogenic efficacies. Related results indicated that TA discoidal rHDL (TA-d-rHDL) maintained similar remodeling behaviors induced by lecithin cholesterol acyl transferase (LCAT) to their native counterparts. However, TA leakage from TA-d-rHDL during the remodeling behaviors would lead to fewer drug distribution in target tissues, verified by near infrared fluorescent *ex vivo* imaging, thus resulting in that antiatherogenic efficacy of TA-d-rHDL was lower than that of TA spherical rHDL (TA-s-rHDL) (6). Analogous problems also persisted in our other previous works, where in the presence of LCAT, d-rHDL loaded with paclitaxel presented faster *in vitro* drug release and lower antitumor efficacy than that in the absence of LCAT (5). Consequently, the development of new methods that can prevent the drug leakage from d-rHDL containing drug during the remodeling behaviors prior to being delivered to the targets would be highly desirable.

The essence of the remodeling behaviors involves that after being activated by apolipoprotein AI (apoAI) bound with d-HDL, LCAT catalyzes the transfer of the sn-2 acyl group of phospholipids into the hydroxyl group of cholesterol to generate cholesterol esters (CE), moreover, CE are sequestered into the center of the d-HDL to form hydrophobic core, ultimately maturing to s-HDL. Among the remodeling behaviors, the essential step is LCAT activation by apoAI in the d-HDL. It has also been demonstrated that reactivity of d-HDL with LCAT would be influenced by the binding extent of apoAI and the negative surface charge of d-HDL (8,9). In our previous studies (10,11), several approaches had been delivered to restraining drug leakage from d-rHDL containing drug during remodeling behaviors induced by LCAT, including d-rHDL constructed by modified-cholesterol, modified-apoAI as well as some special phospholipids or fatty acids. Among them, it was found that d-rHDL mixed with long chain unsaturated fatty acid such as arachidonic acid (AA), 20-carbon chain with four double bonds and negative charge, would increase the fluidity of the phospholipids bilayer of d-rHDL, decrease the insertion extent of apoAI to the phospholipids bilayer and enlarge negative surface charge of d-rHDL. Additionally, AA-d-rHDL represented lower reactivity with LCAT than d-rHDL, which were similar to those results reported by Huggins *et al.* (12) where d-rHDL mixed with long chain polyunsaturated phospholipids exhibited low reactivity with LCAT, and by Sparks *et al.* (13) where intravenous injection of phosphatidylinositol (PI), a phospholipids with negative charge, to New Zealand white rabbits increased negative surface charge of native d-HDL and decreased the production of s-HDL via inhibiting the reactivity of d-HDL with LCAT. So it will be expected that the drug leakage from d-rHDL loaded with drug during the remodeling behaviors could be restrained by AA modification.

Here, based on the endogenous antiatherogenic efficacy and the undesired drug leakage during remodeling behaviors of d-rHDL, the present study was first to develop a novel AA modified-d-rHDL loaded with first-line cholesterol-lowering drug lovastatin (LT). Their *in vitro* physicochemical characterizations such as mean sizes, zeta potentials, EE, DL and apoAI

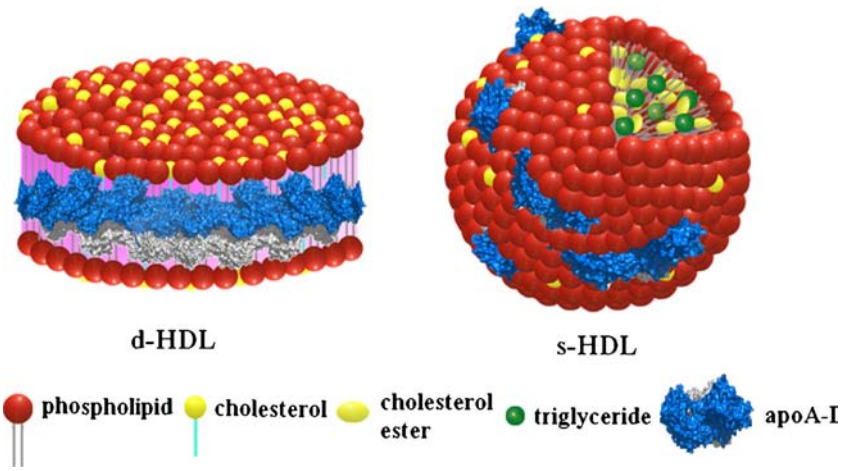

Fig. 1 Diagrammatic sketches of d-HDL and s-HDL.

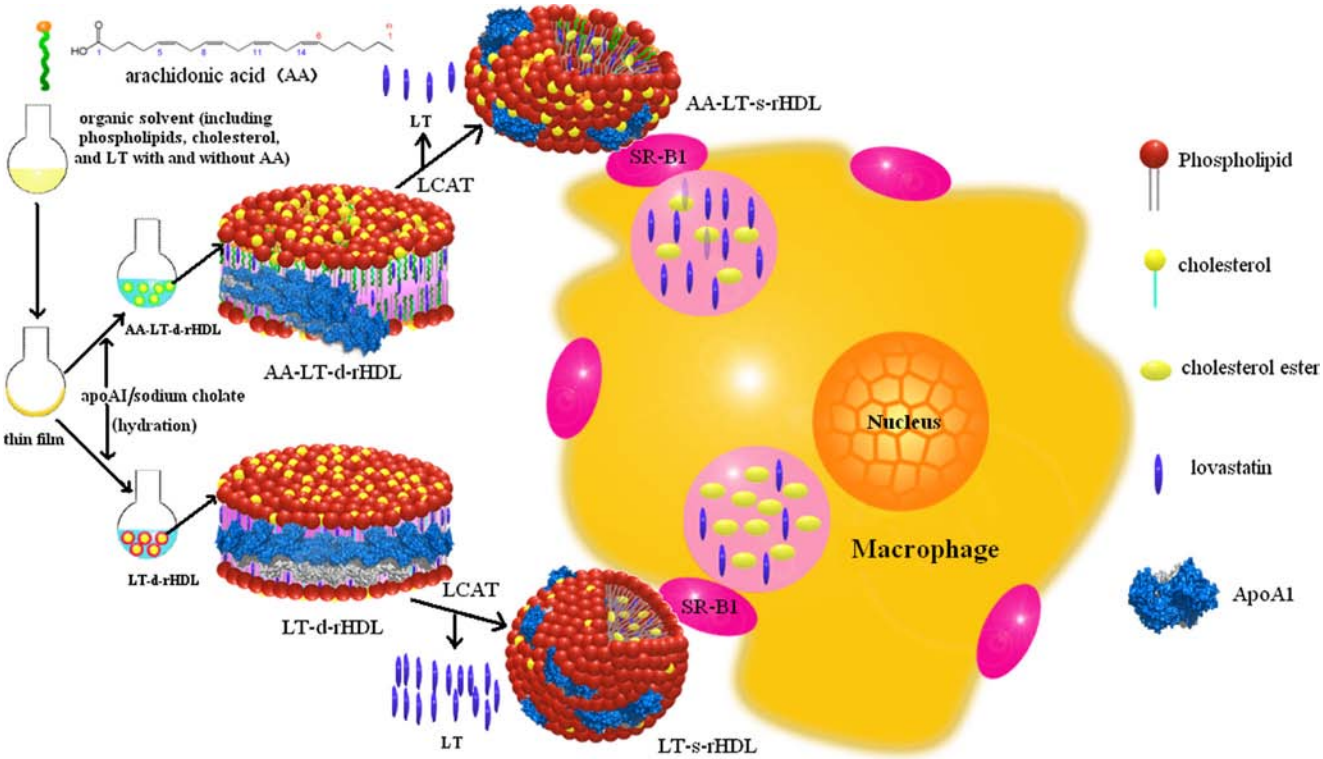

Fig. 2 Schematic diagram on preparation procedures and endocytotic uptake by RAW 264.7.

binding extent were studied, then reactivity of AA-LT-d-rHDL with LCAT was elaborately examined through a series of *in vitro* remodeling behaviors evaluated by change of physicochemical characteristics under the action of LCAT, the structural transformation in the presence of LCAT visualized via transmission electron microscopy (TEM), *in vitro* generation of cholesterol esters (CE) in the presence of LCAT and *in vitro* drug release profiles before and after LCAT addition. Furthermore, the drug efficacies of AA-LT-d-rHDL were comprehensively investigated and compared through inhibition effects on macrophage-derived foam cell formation in the presence of LCAT. The primary aim of this study is to explore whether the AA-LT-d-rHDL have lower reactivity with LCAT and fewer drug leakage during the remodeling behaviors prior to being delivered to the target cells, thus exhibiting stronger inhibition effect on macrophage-derived foam cell formation than LT-d-rHDL in the presence of LCAT. The diagram on our main works was schematically depicted in the Fig. 2.

MATERIALS AND METHODS

Materials

Lovastatin was kindly donated by Jiangsu Yangzi River Pharmacy Company (Taizhou, Jiangsu, China). AA, cholesterol and oil red O were purchased from Sigma-Aldrich (USA). Phospholipids (Lipoid S-100) were obtained from Lipoid GmbH (Germany). 3-(4, 5-dimethylthiazol-2-yl)-2, 5-diphenyltetrazolium bromide (MTT) was purchased from Amersco (Solon, Ohio, USA). oxLDL and DiI-oxLDL were obtained from Guangzhou Yiyuan Biotech. Co. Ltd (Guangzhou, China). The apoAI (97% purity) was isolated from the industrial waste during production of albumin by our laboratory (as described previously).

HPLC-grade reagents were used as the mobile phase in HPLC analysis, and all other reagents were of analytical grade. Distilled and deionized water were used in all experiments.

Preparations

LT-d-rHDL and three AA-LT-d-rHDL preparations were prepared by thin-film dispersion as described previously in those studies (6,14) with minor revisions. Firstly, LT-L and three AA-LT-L preparations were prepared by thin-film dispersion method, respectively. Briefly, 0.4 g Lipoid S-100, different AA modification amount (0/1:20/1:10/1:5, AA: phospholipids mole ratio), 0.04 g cholesterol and 0.02 g LT were dissolved in 30 mL methanol/chloroform (1:1, V/V) and dried in an eggplant-shaped flask under vacuum at 30±2°C. 15 mL of 0.02 M Tris–HCl buffer (pH 8.0) was added into the flask to hydrate the dry film, then the mixture was vortexed thoroughly for 10 min, followed by ultrasonication for 200 s at 300 W on ice using an ultrahomogenizer JY92II (Ningbo, China) until occurrence of clear dispersions. The dispersions

were then filtrated through 0.22 μm filter to remove larger particles.

LT-L and three AA-LT-L preparations obtained above were further incubated with the apoAI to form LT-d-rHDL and three AA-LT-d-rHDL preparations, respectively. Shortly, LT-L and three AA-LT-L preparations were incubated with equivalent volume pH 8.0 Tris–HCl buffer containing 24 mg apoAI and 48 mg sodium cholate under 600 rpm at 4°C for 12 h, then the dispersions were dialyzed against pH 8.0Tris-HCL for 48 h to remove excess sodium cholate.

LT-L obtained above without apoAI incubation was used as normal LT liposomal preparation in the following cell studies.

In Vitro Characterizations

Physicochemical Characteristics Including Mean Sizes, Zeta Potentials, EE and DL

The mean sizes and zeta potentials of LT-d-rHDL and three AA-LT-d-rHDL preparations were measured by dynamic light scattering (DLS) analyzer (Zetasizer 3000 HAS, Malvern, UK). All Samples should be diluted appropriately with aqueous phase before measurement and done in triplicate.

EE and DL were quantified by the micro-column centrifugation method as described previously (6,14). They were determined by HPLC (Shimadzu LC-10A, Kyoto, Japan) equipped with an ultraviolet (UV) detector operated at 238 nm and a shim-pack VP-ODS (150×4.6 mm) column. The mobile phase was methanol/water (76:24, V/V). The flow rate was kept at 1 mL/min and the column temperature was maintained at 30±0.2°C.

EE and DL were calculated as the following formula, where the W means the amount of entrapped LT and W_t means the total LT amount in LT-d-rHDL or three AA-LT-d-rHDL preparations; where the Q means the amount of LT encapsulated in LT-d-rHDL or three AA-LT-d-rHDL preparations, and the Q_t means the total amount of the feeding materials including lipids, apoAI and LT.

$$EE(\%) = \frac{W}{W_t} \times 100\% \tag{1}$$

$$DL(\%) = \frac{Q}{Q_t} \times 100\% \tag{2}$$

In pharmaceutics, concentration of drug carriers is generally defined as the solid content calculated as following formula 3, based on the assumption that all the materials added for the preparation can be basically recovered. As most people do, in our present study, we considered rHDL as drug carrier and concentration of rHDL was calculated by the solid content.

$$Solid\ \ content(mg/mL) = \frac{Total\ \ mass\ \ of\ \ feeding\ \ materials(except\ \ API)}{Volume\ \ of\ \ the\ \ preparation} \tag{3}$$

Effects of AA Modification on apoAI Binding Extent with LT-d-rHDL

Due to the four double bonds in AA, AA insertion would increase the fluidity of phospholipids bilayer and lower the arrangement compactness of phospholipids bilayer, thus probably leading to weak apoAI binding extent with phospholipids bilayer of LT-d-rHDL. Here, guanidine hydrochloride (GdnHCl) denaturation experiment was used to evaluate the apoAI binding extent. Intrinsic fluorescence emission spectra of free apoAI in the solution and apoAI in LT-d-rHDL or three AA-LT-d-rHDL preparations were obtained as depicted previously (14,15). Specifically, GdnHCl solution was prepared in the standard Tris-buffer (pH 8.0) except NaCl and warmed to 25± 0.5°C. 0.5 ml free apoAI solution, LT-d-rHDL and three AA-LT-d-rHDL preparations, also warmed to 25±0.5°C, were added to the GdnHCl solution to obtain the final GdnHCl concentration of 2 M, respectively. The first scan of fluorescence was started 30 s after mixing and completed within 2 min with 280 nm as exciting light. The samples were maintained at 25± 0.5°C and scanned again at 0.5, 1, 2, 4, 6, 10 and 24 h. The fluorescence at each predetermined time point was recorded to examine the denaturation of apoAI.

In Vitro Remodeling Behaviors Evaluation

Physicochemical Characteristics under Action of LCAT

Physicochemical characteristics of LT-d-rHDL and three AA-LT-d-rHDL preparations, including mean sizes, zeta potential, EE and DL, were investigated in the presence of LCAT. Briefly, after being incubated with LCAT for 1 h, LT-d-rHDL and three AA-LT-d-rHDL preparations were subjected to the same determinations described previously in the above 2.3.1.

Structural Transformation under Action of Lcat Visualized by TEM

Similar to the native d-HDL, our previous studies showed that d-rHDL loaded with drug also transformed from the discoidal to the spherical in the remodeling behaviors induced by LCAT (5,10,11). Here, TEM (H-7650, Hitachi High-Technologies Corporation, Japan) was employed to characterize visually the effects of AA modification on the remodeling behaviors of LT-d-rHDL induced by LCAT. Briefly, LT-d-rHDL or three AA-LT-d-rHDL preparations before and after LCAT addition were visualized using TEM as described previously.

Generation of Cholesterol Esters Indicated as Reduced Cholesterol

It is well known that the cholesterol in native d-HDL is esterified into CE catalyzed by LCAT. It has been demonstrated that d-rHDL loaded with drug also had the similar reaction to the native counterparts (5,6). Here, in order to investigate the reactivity of LT-d-rHDL or three AA-LT-d-rHDL preparations with LCAT, the free cholesterol in LT-d-rHDL or three AA-LT-d-rHDL preparations were determined after being incubated with LCAT, and the reduced cholesterol (RC, %) amount was used to indicate the generation of CE. The procedures were the same as described previously (5,6). The generation of CE was indicated as the RC calculated with the following formula, where C_0 was the initial concentration of cholesterol in mixtures, and C_t was the concentration of cholesterol at different time points after incubation of LT-d-rHDL or there AA-LT-d-rHDL preparations with LCAT.

$$RC\% = \frac{C_0 - C_t}{C_0} \times 100\% \tag{4}$$

In Vitro Release

Our previous studies (5,6,10,11) found that the drug leakage from LT-d-rHDL during the remodeling behaviors induced by LCAT would lead much faster drug release due to the free and fast diffusion of leaked free drug. Hence, *in vitro* release experiments were done to investigate influence of AA modification on drug leakage during the remodeling behaviors of LT-d-rHDL induced by LCAT. Briefly, 4 mL of LT-d-rHDL or three AA-LT-d-rHDL preparations with 1 mL LCAT were placed into pre-swollen dialysis bags (8–12 KDa molecular weight cutoffs) respectively, then those dialysis bags were separately immersed in release medium consisting of 200 mL PBS (pH7.4) containing 0.5% SDS as solubilizer, and incubated at 37±0.5°C under a rotation rate of 100 rpm for 72 h. Samples (0.5 mL) were withdrawn at fixed time from release medium during 72 h and refilled with the same volume of fresh medium. Samples were centrifuged at 8,000 rpm for 10 min, and the supernatant were subjected to the HPLC, described above in the section "Physicochemical Characteristics Including Mean Sizes, Zeta Potentials, EE and DL," to calculate the amount of LT in the release medium. The *in vitro* release was expressed by accumulative release (%) at the different time points.

Furthermore, similarity factor f_2 was used as the criterion for assessing similarity between two *in vitro* release profiles of preparation with and without LCAT, and the f_2 was calculated as the following formula.

$$f_2 = 50\log\left\{\left[1 + \frac{1}{n}\sum_{t=1}^{n}(R_{1t} - R_{2t})^2\right]^{-0.5} \times 100\right\} \tag{5}$$

Where the R_{1t} and R_{2t} are the percentage of drug release of LT-d-rHDL and three AA-LT-d-rHDL preparations with and without LCAT at different predetermined time points, respectively; n represents the number of sampling at each time point.

In Vitro Cytotoxicities of Different Blank Drug Carriers and LT Preparations

The *in vitro* cytotoxicities of different blank drug carriers and LT preparations were evaluated by MTT assay (16,17). Specifically, mouse macrophage cell line RAW 264.7 (kindly gifted from Atherosclerosis Research Centre, Nanjing Medical University, Nanjing, PR China) were seeded at a density of 1×10^4 cells/well in 96-well plates and cultured in Dulbecco's Modified Eagle Medium (DMEM) (Sigma, ST. Louis, USA) containing 10% fetal bovine serum (Invitrogen, USA) with 100 units/mL penicillin and 100 μg/mL streptomycin for 24 h at 37±0.5°C in humidified, 5% CO_2 and 95% air. After removing the medium, cells were further incubated with 200 μL fresh medium containing blank liposome (200~1,500 μg/mL), d-rHDL (200~1,500 μg/mL) and three AA-d-rHDL preparations (200~1,500 μg/mL) for 24 h at 37±0.5°C, respectively, to assess the cytotoxicities of blank drug carriers; meanwhile, cells were incubated 200 μL fresh medium containing 20 μM LT solution (LT dissolved in the dimethyl sulfoxide (DMSO) and diluted appropriately before administration), LT-L (20 μM LT), LT-d-rHDL (20 μM LT) and three AA-LT-d-rHDL preparations (20 μM LT), respectively, to assess the cytotoxicities of different six LT preparations.

Subsequently, the 20 μL MTT (5 mg/mL in pH 7.4 PBS) was added into each well, and then cells were stained at 37± 0.5°C for 4 h. Finally, the supernatant was discarded and 150 μL of DMSO was added to dissolve the formed MTT formazan crystals. The absorbance was measured at 570 nm by an ELISA reader (Thermo Scientific, USA). Cell viability (%) was calculated as follows.

$$Cell\ \ viability(\%) = \frac{OD_S - OD_0}{OD_{control} - OD_0} \times 100\% \tag{6}$$

OD_s represents the optical density of wells exposed to the different preparations. $OD_{control}$ represents the optical density of wells treated with supplement-free fresh culture medium, and OD_0 represents the optical density of wells without any treatment. Experiments were performed in triplicate.

Cholesterol Efflux of LT-d-rHDL and Three AA-LT-d-rHDL Preparations from RAW264.7

Cholesterol effluxes from RAW 264.7 treated with different LT-d-rHDL preparations were carried out in order to evaluate the possible antiatherogenic efficacy. The RAW264.7

were seeded at a density of 1×10^5 cells/well in 12-well plates and cultured in DMEM containing 10% fetal bovine serum with 100 units/mL penicillin and 100 μg/mL streptomycin at 37±0.5°C in humidified, 5% CO_2 and 95% air. After 24 h culture, the mediums were discarded and cells were washed by PBS for three times, then cells were added by 200 μL fresh serum-free DMEM containing LT-d-rHDL (20 μM LT), 1:20 AA-LT-d-rHDL (20 μM LT), 1:10 AA-LT-d-rHDL (20 μM LT) or 1:5 AA-LT-d-rHDL (20 μM LT), respectively. After further 24 h incubation, the contents of total cholesterol (TC) and free cholesterol (FC) in the different LT preparations treated-groups were measured by commercial cholesterol quantification kit by Sigma-Aldrich (USA). The cholesterol efflux ability was assessed by TC content and FC content in the RAW 264.7 intervened with different LT preparations, compared with the RAW 264.7 without any intervention (18).

Effects of AA Modification on Cellular Drug Uptake under Action of LCAT

In order to study the effects of LCAT on the cellular drug uptake of different LT preparations and further evaluate the effects of AA modification on the cellular drug uptake of LT-d-rHDL under the action of LCAT, cellular drug uptakes of different LT preparations with and without LCAT were investigated as follows. Specifically, the RAW 264.7 were seeded at a density of 1×10^5 cells/well in 12-well plates and cultured in DMEM containing 10% fetal bovine serum with 100 units/mL penicillin and 100 μg/mL streptomycin at 37± 0.5°C in humidified, 5% CO_2 and 95% air. After 24 h culture, the mediums were discarded and cells were washed by PBS for three times, then cells were further incubated by fresh serum-free DMEM, containing 120 μg/mL oxidized low density lipoproteins (oxLDL) and 20 μM LT of different preparations with or without 200 μL LCAT, respectively. Different LT preparations were LT-L, LT-d-rHDL 1:20 AA-LT-d-rHDL, 1:10 AA-LT-d-rHDL and 1:5 AA-LT-d-rHDL, respectively. The dose of LT in all LT preparations was 20 μM.

After 24 h incubation, the mediums were removed and cells were rinsed with PBS for 3 times to remove the excessive non-phagocytosed carriers. In order to extract the drug from cells, the washed cells were collected in the 40 μL PBS and subject to five freezing-thawing cycles to split the cells, then 5 μL cell lysates were used to determine total cell proteins using Pierce BCA assay (Pierce, Cramlington, U.K.) and the rest of cell lysates were added by 200 μL methanol to extract the LT. After centrifugation at 8,000 rpm for 10 min, the LT in the supernatant was determined using the HPLC method described above. The amount of LT uptake was expressed as drug uptake (drug content/protein, ng/ng) to eliminate the difference induced by different cell numbers in each well (19).

Inhibition Effects of Different LT Preparations on Macrophage-Derived Foam Cell Formation in the Presence of LCAT

Preventive administration was used as the dosage regimen to examine the inhibition effect of different LT preparations on macrophage-derived foam cell formation in the presence of LCAT. Specifically, RAW 264.7 were seeded at a density of 1×10^5 cells/well in 12-well plates and cultured in DMEM containing 10% fetal bovine serum with 100 units/mL penicillin and 100 μg/mL streptomycin at 37±0.5°C in humidified, 5% CO_2 and 95% air. After 24 h culture, the mediums were discarded and cells were washed by PBS for three times, then fresh serum-free DMEM, containing 120 μg/mL oxLDL, 200 μL LCAT and 20 μM LT of different LT preparations, were added into cells, respectively. According to the different LT preparations, intervened groups could be divided into the following 6 groups: 20 μM LT-S (LT dissolved in the DMSO and diluted appropriately before administration, defined as group C), LT-L (20 μM LT, defined as group D), LT-d-rHDL (20 μM LT, defined as group E), 1:20 AA-LT-d-rHDL (20 μM LT, defined as group F), 1:10 AA-LT-d-rHDL (20 μM LT, defined as group G) and 1:5 AA-LT-d-rHDL (20 μM LT, defined as group H), respectively. Besides, cells then cultured by fresh serum-free DMEM were taken as normal control group (defined as group A), while cells cultured by fresh serum-free DMEM only containing 120 μg/mL oxLDL were taken as positive control group (defined as group B). After further being cultured for a period of time, all the groups were subject to the following examinations in order to elaborately compare and evaluate the inhibition effects of different LT preparations on macrophage-derived foam cell formation in the presence of LCAT, respectively (7,20).

Intracellular Lipid Dispositions Stained by Oil Red O

After 24 h incubation, cells were washed three times with PBS and fixed in 4% paraformaldehyde for 10 min. After being rinsed with PBS for 3 times, cells were stained with 0.5% oil red O in 60% isopropanol for 1 h, and then washed with 60% isopropanol. After being washed with PBS, cells were immersed in PBS, then morphologically evaluated by microscope (IX71; Olympus, Japan) at ×400 magnifications (21,22), respectively.

The positive staining area (%) was used as an indicator of the extent of intracellular lipid deposition, which was quantified by using Image-Pro Plus 6.

Determination of Intracellular Cholesterol Esters Content

It is universally known that the intracellular CE content is a quantitative sign of foam cell formation. So the intracellular CE contents in the different cell groups were determined to

evaluate the progress of macrophage-derived foam cell, respectively. Specifically, after 24 h incubation, cellular CE content was determined. Specifically, cells were washed by PBS for three times, then total cholesterol (TC) and free cholesterol (FC) content in cells were determined by the commercial cholesterol quantification kit by Sigma-Aldrich (USA), respectively. According to the standard protocol of the kit, intracellular CE content were calculated by subtracting the value of cellular FC from the value of cellular TC as the following formula. Moreover, total cell proteins were determined using Pierce BCA assay (Pierce, Cramlington, U.K.). Results of cellular CE content were expressed as μg/mg protein (23).

$$CE = TC - FC \tag{7}$$

DiI-oxLDL Uptake

To visually examine oxLDL uptake by RAW 264.7 cells, DiI-oxLDL substituted for oxLDL was used to induce cell to form foam cell. Briefly, cells were cultured and intervened as previously described above only except replacing oxLDL by DiI-oxLDL. After 24 h incubation, cells were washed by PBS for three times to remove the non-phagocytosed DiI-oxLDL, and fixed in 4% paraformaldehyde for 20 min, then cells were labeled by DAPI, examining by confocal microscopy (LSM 710; Carl Zeiss Q10, Germany) (24).

To evaluate quantitatively the cellular uptake of DiI-oxLDL, the mean fluorescence intensity of each cell group was detected by flow cytometry (FACSCalibur, Becton Dickinson, USA). Briefly, after 24 h incubation, cells were rinsed by PBS for 3 times to remove the non-phagocytosed DiI-oxLDL, and then collected in the PBS. Moreover, the collected cells were shaken fully to disperse cells in PBS and then subject to centrifugation in order to further remove the non-phagocytosed DiI-oxLDL on the surface of cells. After five dispersion-centrifugation cycles, the re-dispersed cells in PBS were detected under flow cytometry (25).

RT-PCR and ELISA Assays for IL-6 and TNF-α

Due to the fast expression and subsequent transcription of mRNA, real-time PCR was carried out to detect the RNA levels of inflammatory cytokines in each cell group after 6 h culture. Specifically, total RNA was extracted with the RNeasy RNA isolation kit (Qiagen, Germany). 0.5 μg of total RNA was used as template to synthesize cDNA using a first strand synthesis kit (Invitrogen, San Diego, CA, USA). Real-time PCR reactions were carried out on the ABI Prism 7500 system (Applied Biosystems, Foster City, CA, USA). Primers and Taqman probes used for real-time reactions were bought from Applied Biosystems. Cytokine RNA levels were analyzed by normalizing with reduced glyceraldehydes-phosphate dehydrogenase (GAPDH) RNA expression (26).

Specifically, the primer pairs were used as: TNF-α, 5′-GGC TGT ACC TCA TCT ACT CC-3′ (forward), 5′-CAG CAA GTC CAG ATA GTC G-3′ (reverse); IL-6, 5′-GTG AGA AGT ATG AGA AGT GTG A-3′ (forward), 5′-GCA GGA TGA GAA TGA TCT TG-3′ (reverse); GAPDH, 5′-ACG ACC ATG GAG AAG GCT G-3′ (forward), 5′-TCG TAC GAG GAA ATG AGC T-3′ (reverse). PCR amplification was performed in duplicate using 96-well plates and the PCR cycling conditions were as follows: 50 C for 2 min and 95 C for 10 min followed by 40 cycles (95 C for 15 s, 60 C for 1 min). GAPDH was used as a reference gene. All samples were normalized to the GAPDH values and the results expressed as fold changes of cycle threshold (C_T) value relative to controls using the $2^{-\Delta\Delta CT}$ formula, and the ΔΔCT was calculated as follows.

$$\Delta\Delta C_T = \left(C_T - C_{reference}\right)_{test} - \left(C_T - C_{reference}\right)_{control} \tag{8}$$

where $(C_T - C_{reference})_{test}$ indicates the difference between C_T for target gene and C_T for reference gene in intervened groups, and $(C_T - C_{reference})_{control}$ indicates the difference between C_T for target gene and C_T for reference gene in normal control group.

Meanwhile, in order to determine the concentrations of IL-6 and TNF-α in cell culture mediums, after 24 h incubation, the cell culture mediums were collected and centrifuged at 12,000 rpm for 10 min at 4°C, and then assessed by ELISA (Biosource, Camarillo, CA, USA) according to the manufacturer's protocol (27).

RT-PCR and Western Blot Analyses for CD36

The mRNA levels of CD36 in different intervened-groups were also detected by RT-PCR as described previously in the RT-PCR for IL-6 and TNF-α, and the primer pairs for CD36 were used as: 5′-GAT GGC CTT ACT TGG GAT TGG-3′ (forward) and 5′-TTT ACC AAA GAT GTA GCC AGT G-3′ (reverse) (28).

Western blot analysis was performed to examine CD36 expression after 24 h culture. Whole-cell lysates were obtained by re-suspending cell pellets in RIPA buffer (50 mM Tris pH 7.4, 150 Mm NaCl, 1% Triton X-100) with freshly added protease inhibitor (Roche). After the lysis proceeded for 30 min on ice, the cell protein concentration was determined using the Pierce BCA protein assay kit. Specifically, the protein extracts (40 μg) were treated with 5×sodium dodecyl sulfate (SDS)-PAGE sample buffer (0.35 mol/L Tris–HCl, pH 6.8, 15% SDS, 56.5% glycerol, 0.0075% bromophenol blue), and then heated at 100°C for 5 min and separated by electrophoresis on a 8% SDS-polyacrylamide gel. The proteins were then transferred onto PVDF Membranes (Merck

Millipore, USA). The Membrane were blocked with 5% skim milk in TBST buffer (0.05% Tween 20, pH 7.5) for 2 h and incubated overnight at 4°C with the rabbit polyclonal antibody against CD36 (1:800, sr-9154, Santa Cruz Biotechnology, Inc. USA), then washed three times with TBST and incubated at room temperature for 1 h with corresponding secondary antibodies such as goat anti-rabbit horseradish peroxidase-conjugated secondary antibody for CD36 (1:3000, sigma, USA). After being washed with TBST for three times, the signals were detected with the electrochemiluminescence (ECL) system (Amersham, UK) and quantified by scanning densitometry with the Image J software. Furthermore, densitometry was analyzed and expressed as fold change relative to beta-actin (internal control protein purchased from Sigma) (29).

Statistical Analysis

Data were expressed as mean ± standard deviation (SD) from individual magnitudes. Statistical analysis was performed by student's *t*-test for two groups, and one-way ANOVA for multiple groups, and the differences were considered to be significant when $P<0.05$.

RESULTS

In Vitro Characterizations

Physicochemical Characteristics Including Mean Sizes, Zeta Potentials, EE and DL

The mean sizes, zeta potentials, EE (%) and DL (%) of LT-d-rHDL and three AA-LT-d-rHDL preparations, analyzed by DLS analyzer and HPLC assay, were given specifically in the following Table I. We could know that as AA modification amount increased, both mean size and negative surface charge of nanocarriers were markedly increased. Specifically, the mean sizes of LT-d-rHDL, 1:20 AA-LT-d-rHDL, 1:10 AA-LT-d-rHDL and 1:5 AA-LT-d-rHDL were found to be 43.2 ± 1.2 nm, 52.7 ± 0.8 nm, 55.6 ± 2.1 nm and 58.3 ± 0.9 nm, respectively (among them, $p<0.05$, compared 1:20 AA-d-rHDL with LT-d-rHDL and $p<0.05$, compared 1:5 AA-d-rHDL with 1:10 AA-d-rHDL); moreover, the corresponding zeta potentials were −12.15 ± 1.07 mV, −20.23 ± 2.42 mV, −24.21 ± 1.12 mV and −29.52 ± 3.21 mV, respectively ($p<0.05$, compared 1:20 AA-d-rHDL with LT-d-rHDL, $p<0.05$, compared 1:10 AA-d-rHDL with 1:20 AA-d-rHDL and $p<0.05$, compared 1:5 AA-d-rHDL with 1:10 AA-d-rHDL, respectively). But the EE and DL were not significantly changed with the increment of AA modification amount. To be more precise, the EE and DL of LT-d-rHDL, 1:20 AA-LT-d-rHDL, 1:10 AA-LT-d-rHDL and 1:5 AA-LT-d-rHDL were 91.2 ± 0.7% and 4.2 ± 0.3%, 90.7 ± 0.5% and 4.1 ± 0.3%, 90.3 ± 0.2% and 4.0 ± 0.2%, and 90.1 ± 0.3% and 3.9 ± 0.1%, respectively.

Meanwhile, concentrations of drug carriers in our studies such as liposome, d-rHDL, 1:20 AA-d-rHDL, 1:10 AA-d-rHDL and 1:5 AA-d-rHDL, calculated by solid content (mg/mL), were 14.7 mg/mL, 15.5 mg/mL, 15.7 mg/mL, 16.0 mg/mL and 16.5 mg/mL, respectively.

Effects of AA Modification on apoAI Binding Extent with LT-d-rHDL

The results in Fig. 3 showed that unfoldings of apoAI in solution and four different LT preparations under the action of GdnHCl, indicated as the maximum denaturation fluorescence (MDF) after 24 h incubation with GdnHCl. As known from the figure, compared with free apoAI solution, the MDF (nm) in the LT-d-rHDL had been significantly reduced ($p<0.05$, compared apoAI in the free apoAI solution *vs.* apoAI in the LT-d-rHDL); moreover, with the increment of AA modification amount, the MDF had been increased gradually followed as LT-d-rHDL, 1:10 AA-LT-d-rHDL, 1:20 AA-LT-d-rHD and 1:10 AA-LT-d-rHDL, respectively (specifically, $p<0.05$, compared apoAI in the 1:20 AA-LT-d-rHDL *vs.* apoAI in the LT-d-rHDL, $p<0.05$, compared apoAI in the 1:10 AA-LT-d-rHDL *vs.* apoAI in the 1:20 AA-LT-d-rHDL and $p<0.05$, compared apoAI in the 1:5 AA-LT-d-rHDL *vs.* apoAI in the 1:10 AA-LT-d-rHDL, respectively).

Table I Mean Sizes, Zeta Potential, EE and DL in the Absence of LCAT (Mean Value ± SD, $n=3$)

	LT-d-rHDL	1:20 AA-LT-d-rHDL	1:10 AA-LT-d-rHDL	1:5 AA-LT-d-rHDL
Mean size (nm)	43.2 ± 1.2	52.7 ± 0.8§	55.6 ± 2.1	58.3 ± 0.9●
Zeta potential (mV)	-12.15 ± 1.07	-20.23 ± 2.42§	-24.21 ± 1.12◆	-29.52 ± 3.21●
EE (%)	91.2 ± 0.7	90.7 ± 0.5	90.3 ± 0.2	90.1 ± 0.3
DL (%)	4.2 ± 0.3	4.1 ± 0.3	4.0 ± 0.2	3.9 ± 0.1

Significant differences: §$p<0.05$, compared 1:20 AA-LT-d-rHDL with LT-d-rHDL; ◆$p<0.05$, compared 1:10 AA-LT-d-rHDL with 1:20 LT-d-rHDL; ●$p<0.05$, compared 1:5 AA-LT-d-rHDL with 1:10 LT-d-rHDL

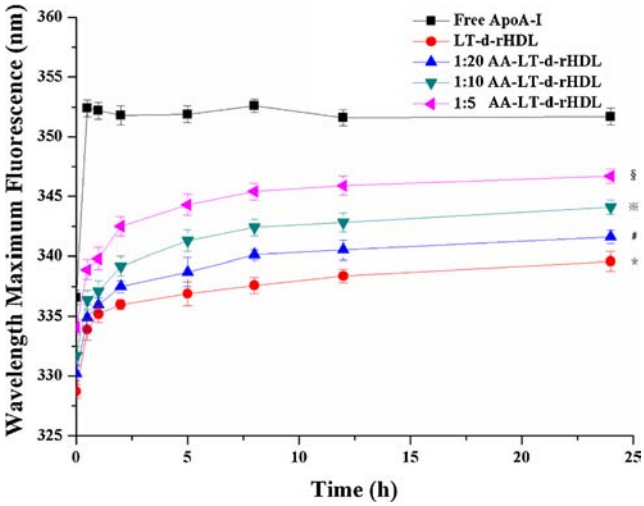

Fig. 3 Influence of GdnHCl on the fluorescence emission spectrum of free apoAI in solution, apoAI in LT-d-rHDL and apoAI in three AA-LT-d-rHDL preparations; Significant differences: *$p<0.05$, compared MDF of apoAI in LT-d-rHDL with that in apoAI solution, #$p<0.05$, compared MDF of apoAI in 1:20 AA-LT-d-rHDL with that in LT-d-rHDL, ※$p<0.05$, compared MDF of apoAI in 1:10 AA-LT-d-rHDL with that in 1:20 AA-LT-d-rHDL, §$p<0.05$, compared MDF of apoAI in 1:5 AA-LT-d-rHDL with that in 1:10 AA-LT-d-rHDL (mean value ± SD, $n=3$).

In Vitro Remodeling Behaviors Evaluation

Physicochemical Characteristics under Action of LCAT

As depicted in the Table II, the mean sizes (nm) and EE (%) of all four different preparations had been distinctly changed after incubation with LCAT, compared with those before incubation with LCAT (listed in the above Table I). Specifically, the mean sizes of all four different preparations with LCAT became larger than those without LCAT ($p<0.05$, compared LT-d-rHDL in the presence of LCAT with that in the absence of LCAT, $p<0.05$, compared 1:20 AA-LT-d-rHDL in the presence of LCAT with that in the absence of LCAT, $p<0.05$, compared 1:10 AA-LT-d-rHDL in the presence of LCAT with that in the absence of LCAT and $p<0.05$, compared 1:5 AA-LT-d-rHDL in the presence of LCAT with that in the absence of LCAT, respectively); moreover, the EE of all four different preparations with LCAT became lower than those without LCAT ($p<0.05$, compared LT-d-rHDL in the presence of LCAT with that in the absence of LCAT, $p<0.05$, compared 1:20 AA-LT-d-rHDL in the presence of LCAT with that in the absence of LCAT, $p<0.05$, compared 1:10 AA-LT-d-rHDL in the presence of LCAT with that in the absence of LCAT and $p<0.05$, compared 1:5 AA-LT-d-rHDL in the presence of LCAT with that in the absence of LCAT, respectively); furthermore, with the increment of AA modification amount, the EE had been increasingly enlarged in the presence of LCAT (specifically, in the presence of LCAT, $p<0.05$, compared 1:20 AA-LT-d-rHDL with LT-d-rHDL, $p<0.05$, compared 1:10 AA-LT-d-rHDL with 1:20 AA-LT-d-rHDL and $p<0.05$, compared 1:5 AA-LT-d-rHDL with 1:10 AA-LT-d-rHDL, respectively).

Structural Transformation under Action of LCAT Visualized by TEM

It was known from Fig. 4 that LT-L and three AA-LT-L preparations had liposomal-like structure (Fig. 4A1-D1), after incubation with apoAI, which were converted into the multi-discoidal (Fig. 4A2-D2) similar to the native counterpart in circulation. Moreover, there were no distinct structural differences between LT-d-rHDL and three AA-LT-d-rHDL preparations in the absence of LCAT, and the sizes were basically consistent with those results obtained by DLS analyzer. The structural conversion from the multi-discoidal to the spherical during remodeling behaviors induced by LCAT were characterized in Fig. 4A3-D3, which indicated that LT-d-rHDL and three AA-LT-d-rHDL preparations maintained the remodeling behaviors under the action of LCAT similar to the metabolic process of native HDL. Moreover, those pictures also suggested that with the increment of AA modification amount, three AA-LT-d-rHDL preparations showed weaker remodeling behaviors induced by LCAT, thus presenting more multi-discoidal marked by the red arrow and less spherical structure (Fig. 4A3-D3). In detail, the number of the red arrow progressively increased followed as LT-d-rHDL, 1:20 AA-LT-d-

Table II Mean Sizes, Zeta Potential, EE and DL in the Presence of LCAT (Mean Value ± SD, $n=3$)

	LT-d-rHDL	1:20 AA-LT-d-rHDL	1:10 AA-LT-d-rHDL	1:5 AA-LT-d-rHDL
Mean size (nm)	88.4 ± 5.7●	82.6 ± 3.8#	75.5 ± 4.3*	69.2 ± 4.9◇
Zeta potential (mV)	−11.33 ± 2.32	−19.61 ± 3.55	−22.37 ± 3.16	−27.48 ± 3.03
EE (%)	54.4 ± 3.2●	65.3 ± 2.7§#	74.4 ± 1.6※*	82.6 ± 3.1◆◇
DL (%)	2.4 ± 0.5	2.9 ± 0.4	3.2 ± 0.2	3.6 ± 0.1

Significant differences: ●$p<0.05$, compared LT-d-rHDL in the presence of LCAT with that in the absence of LCAT; #$p<0.05$, compared 1:20 AA-LT-d-rHDL in the presence of LCAT with that in the absence of LCAT; *$p<0.05$, compared 1:10 AA-LT-d-rHDL in the presence of LCAT with that in the absence of LCAT; ◇$p<0.05$, compared 1:5 AA-LT-d-rHDL in the presence of LCAT with that in the absence of LCAT; §$p<0.05$, compared 1:20 AA-LT-d-rHDL in the presence of LCAT with LT-d-rHDL in the presence of LCAT; ※$p<0.05$, compared 1:10 AA-LT-d-rHDL in the presence of LCAT with 1:20 AA-LT-d-rHDL in the presence of LCAT; ◆$p<0.05$, compared 1:5 AA-LT-d-rHDL in the presence of LCAT with 1:10 AA-LT-d-rHDL in the presence of LCAT

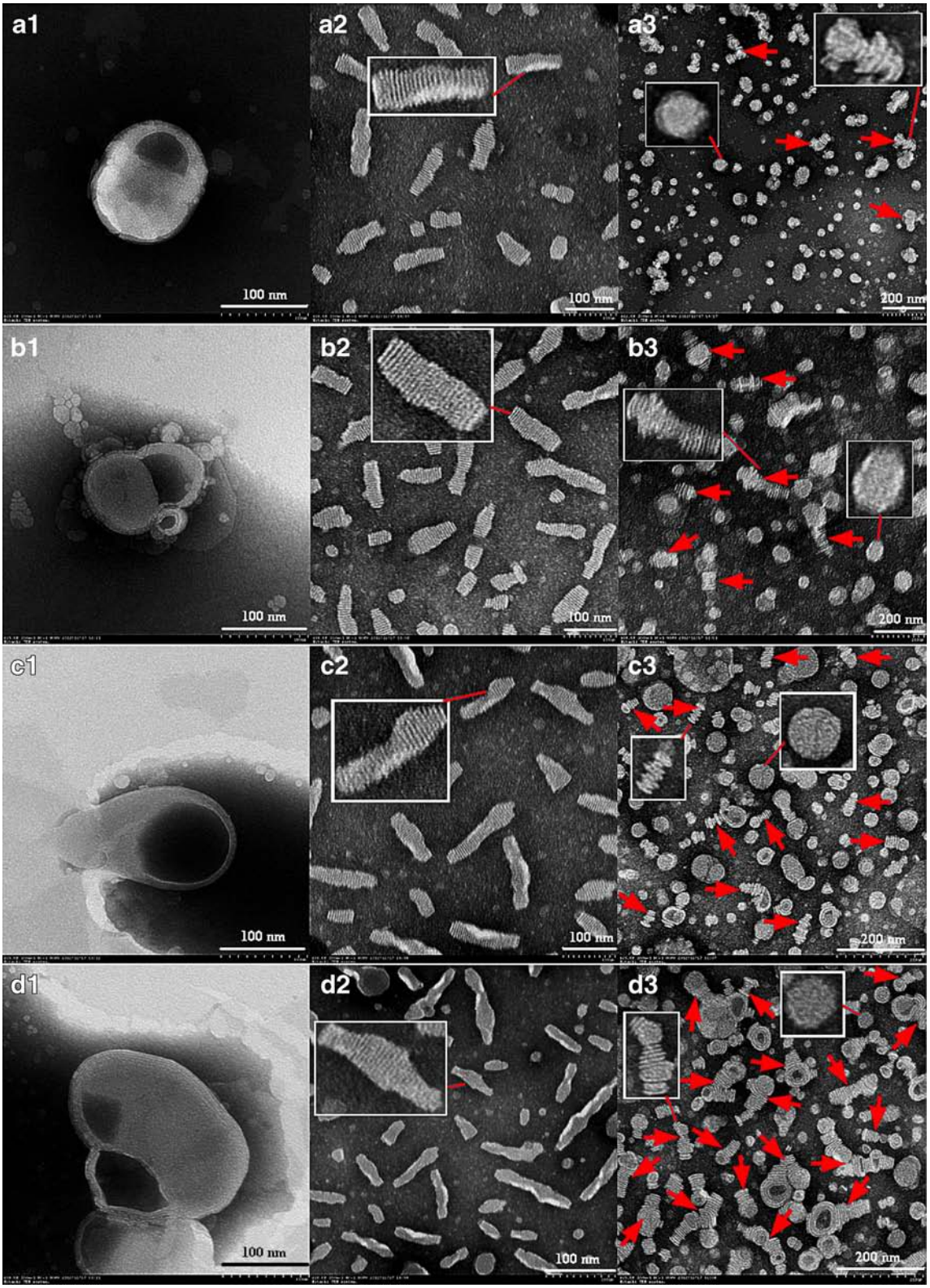

Fig. 4 Photographs visualized by TEM. (**a1**-**d1**) show LT-L (**a1**), 1:20 AA-LT-L (**b1**), 1:10 AA-LT-L (**c1**) and 1:5 AA-LT-L (**d1**), respectively. (**a2**-**d2**) show LT-d-rHDL (**a2**), 1:20 AA-LT-d-rHDL (**b2**), 1:10 AA-LT-d-rHDL (**c2**) and 1:5 AA-LT-d-rHDL (**d2**) in the absence of LCAT, respectively. (**a3**-**d3**) show LT-d-rHDL (**a3**), 1:20 AA-LT-d-rHDL (**b3**), 1:10 AA-LT-d-rHDL (**c3**) and AA-1:5 LT-d-rHDL (**d3**) in the presence of LCAT, respectively. The *red slim lines* mean the magnified zones, and the *red arrows* mean the reversed discoidal fragments after incubation with LCAT.

rHDL, 1:10 AA-LT-d-rHDL, 1:5 AA-LT-d-rHDL, respectively.

Generation of Cholesterol Esters Indicated as Reduced Cholesterol

For all the four different preparations, RC (%) at each predetermined time point, as the indicator of CE generation catalyzed by LCAT, were depicted in the following Fig. 5. It could be drawn from the figure that AA modification would inhibit the reduction of cholesterol catalyzed by LCAT. In other words, the more AA amount was inserted, the less CE was generated. Specifically, after 24 h incubation, the RC of LT-d-rHDL, 1:20 AA-LT-d-rHDL, 1:10 AA-LT-d-rHDL and 1:5 AA-LT-d-rHDL were 41.1±1.5%, 38.4±1.4%, 33.7±0.5% and 30.4±1.4%, respectively (specifically, $p<0.05$ for 1:20 AA-LT-d-rHDL *vs.* LT-d-rHDL, $p<0.05$ for 1:10 AA-LT-d-rHDL *vs.* 1:20 AA-LT-d-rHDL and $p<0.05$ for 1:5 AA-LT-d-rHDL *vs.* 1:10 AA-LT-d-rHDL).

In Vitro Release

In vitro release profiles of LT-d-rHDL and three AA-LT-d-rHDL preparations with and without LCAT were plotted in the Fig. 6.

In the absence of LCAT, accumulative drug release (%) after 72 h was slightly augmented with increment of AA modification amount, respectively, and among there was significant difference between 1:5 AA-LT-d-rHDL and LT-d-rHDL ($p<0.05$ for 1:5 AA-LT-d-rHDL *vs.* LT-d-rHDL).

In the presence of LCAT, accumulative drug releases of all four preparations became bigger than those in the absence of

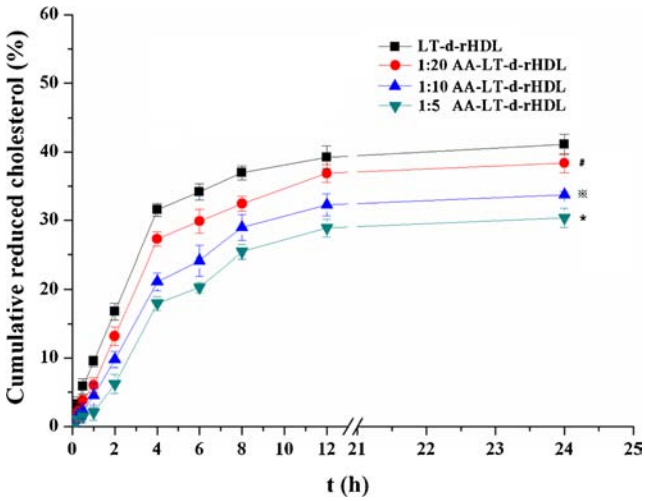

Fig. 5 *In vitro* cumulative reduced cholesterol (%) in LT-d-rHDL and three AA-LT-d-rHDL preparations after incubation with LCAT at the predetermined time points; Significant differences: #$p<0.05$, compared 1:20 AA-LT-d-rHDL with LT-d-rHDL after 24 h, ※$p<0.05$, compared 1:10 AA-LT-d-rHDL with 1:20 AA-LT-d-rHDL after 24 h, *$p<0.05$, compared 1:5 AA-LT-d-rHDL with 1:10 AA-LT-d-rHDL after 24 h (mean value ± SD, $n=3$).

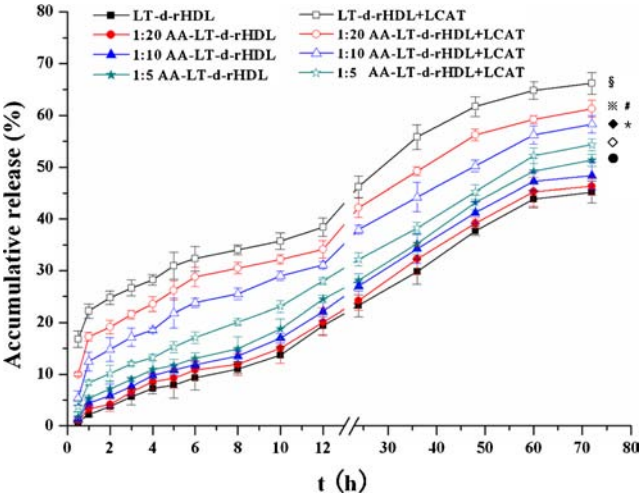

Fig. 6 *In vitro* release profiles of LT-d-rHDL and different AA-LT-d-rHDL preparations with and without LCAT; Significant differences: ●$p<0.05$, compared 1:5 AA-LT-d-rHDL with LT-d-rHDL in the absence of LCAT after 72 h, §$p<0.05$, compared LT-d-rHDL in the presence of LCAT with that in the absence of LCAT after 72 h, ※$p<0.05$, compared 1:20 LT-d-rHDL in the presence of LCAT with that in the absence of LCAT after 72 h, ◆$p<0.05$, compared 1:10 LT-d-rHDL in the presence of LCAT with that in the absence of LCAT after 72 h, #$p<0.05$, compared 1:20 LT-d-rHDL with LT-d-rHDL in the presence of LCAT after 72 h, *$p<0.05$, compared 1:10 LT-d-rHDL with 1:20 LT-d-rHDL in the presence of LCAT after 72 h, ◇$p<0.05$, compared 1:5 LT-d-rHDL with that of 1:10 LT-d-rHDL in the presence of LCAT after 72 h (mean value ± SD, $n=3$).

LCAT (specifically, $p<0.05$ for LT-d-rHDL in the absence of LCAT *vs.* LT-d-rHDL in the presence of LCAT, $p<0.05$ for 1:20 AA-LT-d-rHDL in the absence of LCAT *vs.* 1:20 AA-LT-d-rHDL in the presence of LCAT and $p<0.05$ for 1:10 AA-LT-d-rHDL in the absence of LCAT *vs.* 1:10 AA-LT-d-rHDL in the presence of LCAT, respectively); moreover, in the presence of LCAT, accumulative drug releases of preparations were further reduced with the increment of AA modification amount (under the action of LCAT, specifically, $p<0.05$ for 1:20 AA-LT-d-rHDL *vs.* LT-d-rHDL, $p<0.05$ for 1:10 AA-LT-d-rHDL *vs.* of 1:20 LT-d-rHDL and $p<0.05$ for 1:5 AA-LT-d-rHDL *vs.* of 1:10 LT-d-rHDL, respectively).

In addition, similarity factor f_2 examination also demonstrated that with AA modification increment, f_2 of *in vitro* release profiles with and without LCAT became larger, which further meant that the difference between *in vitro* release profiles with and without LCAT became smaller, especially for *in vitro* release profiles of 1:5 AA-LT-d-rHDL with and without LCAT. Specifically, f_2 of *in vitro* release profiles with and without LCAT including LT-d-rHDL, 1:20 AA-LT-d-rHDL, 1:10 AA-LT-d-rHDL and 1:5 AA-LT-d-rHDL were 33.13±1.93, 40.08±3.82, 50.29±2.51and 68.43±3.07, respectively.

In Vitro Cytotoxicities of Different Blank Drug Carriers and LT Preparations

Results on the toxicity of various blank drug carriers were displayed in Fig. 7. No obvious cytotoxicities were observed

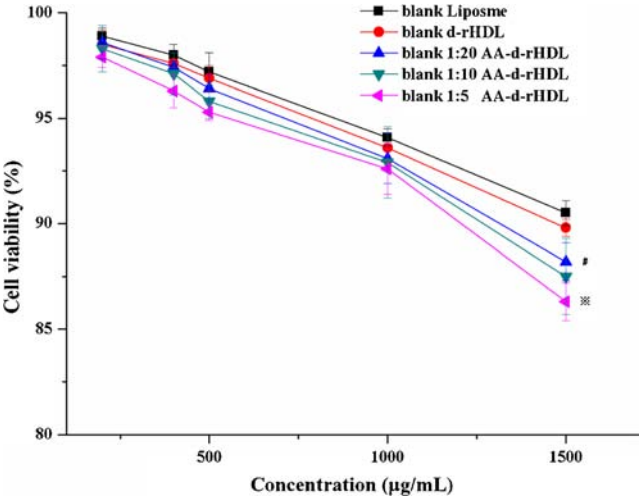

Fig. 7 *In vitro* cytotoxicities of blank drug carriers including liposome, d-rHDL, 1:20 AA-d-rHDL, 1:10 AA-d-rHDL and 1:5 AA-d-rHDL on RAW 264.7 at different concentrations ranging from 200 to 1,500 μg/mL; Significant differences: #$p<0.05$, compared 1:20 AA-d-rHDL with d-rHDL when the concentrations reached to 1,500 μg/mL, ※$p<0.05$, compared 1:5 AA-d-rHDL with 1:20 AA-d-rHDL when the concentrations reached to 1,500 μg/mL (mean value ± SD, $n=3$).

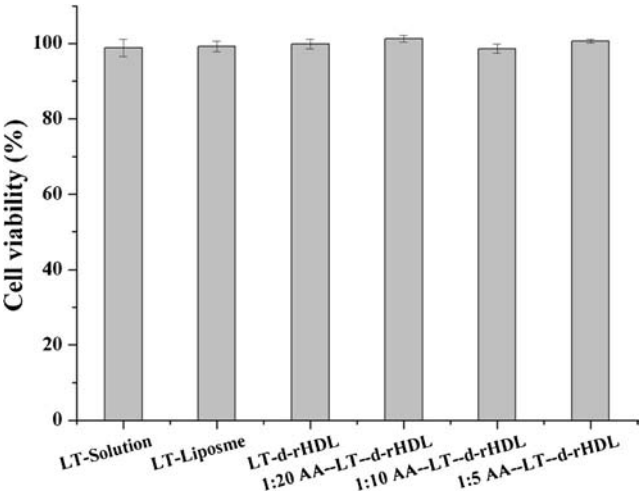

Fig. 8 *In vitro* cytotoxicities of LT-L, LT-d-rHDL, 1:20 AA-LT-d-rHDL, 1:10 AA-LT-d-rHDL and 1:5 AA-LT-d-rHDL on RAW 264.7 at the concentrations same as used in the following cell studies (mean value ± SD, $n=3$), among in all intervened-groups concentrations of LT were 20 μM and concentrations of drug carriers (expressed as solid content, μg/mL) including liposome, d-rHDL, 1:20 AA-d-rHDL, 1:10 AA-d-rHDL and 1:5 AA-d-rHDL were 198.1 μg/mL, 208.8 μg/mL, 212.4 μg/mL, 216.2 μg/mL and 223.2 μg/mL, respectively.

for any drug carriers in the concentrations from 200 to 500 μg/mL, and slight reduction in cell viability occurred when the concentrations were above 500 μg/mL. When the concentrations of blank drug carriers reached 1,500 μg/mL, significant differences on cytotoxicity were seen in the groups treated with three blank AA-d-rHDL preparations, compared with blank d-rHDL and blank liposome (specifically, $p<0.05$ for blank 1:20 AA-d-rHDL *vs.* blank d-rHDL and $p<0.05$ for blank 1:5 AA-d-rHDL *vs.* blank 1:20 AA-d-rHDL).

Meanwhile, no obvious cytotoxicities were perceived for any LT preparations at the concentration of 20 μM LT, compared with the normal control cell (seen from Fig. 8).

Cholesterol Efflux of LT-d-rHDL and Three AA-LT-d-rHDL Preparations from RAW264.7

Intracellular TC contents and FC contents in different groups after 24 h culture were depicted in the Fig. 9, and there were no significant difference among groups. Specifically, intracellular TC contents (TC content/protein, μg/mg) in the different groups were 37.7 ± 2.1 μg/mg in the normal control RAW 264.7 cells, 35.8 ± 2.0 μg/mg in the cells treated with LT-d-rHDL, 36.2 ± 1.7 μg/mg in the cells treated with 1:20 AA-LT-d-rHDL, 36.7 ± 1.4 μg/mg in the cells treated with 1:10 AA-LT-d-rHDL and 37.1 ± 1.2 μg/mg in the cells treated with 1:5 AA-LT-d-rHDL, respectively; intracellular FC contents (FC content/protein, μg/mg) in the different groups were 32.2 ± 1.7 μg/mg in the normal control cells, 29.8 ± 1.5 μg/mg in the cells treated with LT-d-rHDL, 30.4 ± 1.1 μg/mg in the cells treated with 1:20 AA-LT-d-rHDL, 30.7 ± 1.7 μg/mg in the cells treated with 1:10 AA-LT-d-rHDL and 31.2 ± 0.9 μg/mg in the cells treated with 1:5 AA-LT-d-rHDL, respectively.

Effects of AA Modification on Cellular Drug Uptake under Action of LCAT

Seen from Fig. 10, in the absence of LCAT, cellular drug uptake (drug content/protein, ng/ng) of LT-L was higher than that of LT-S ($p<0.05$ for LT-S *vs.* LT-L); moreover, cellular drug uptake of LT-d-rHDL was much higher than

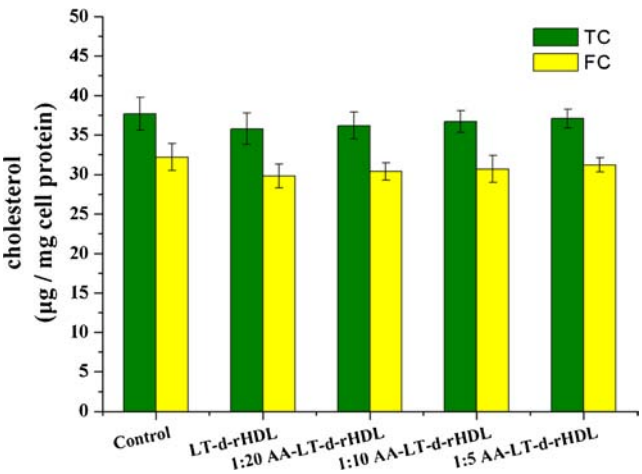

Fig. 9 Cholesterol effluxes from RAW 264.7 treated with different LT-d-rHDL preparations (mean value ± SD, $n=6$), among in all intervened-groups concentrations of LT were 20 μM and concentrations of drug carriers (expressed as solid content, μg/mL) including liposome, d-rHDL, 1:20 AA-d-rHDL, 1:10 AA-d-rHDL and 1:5 AA-d-rHDL were 198.1 μg/mL, 208.8 μg/mL, 212.4 μg/mL, 216.2 μg/mL and 223.2 μg/mL, respectively.

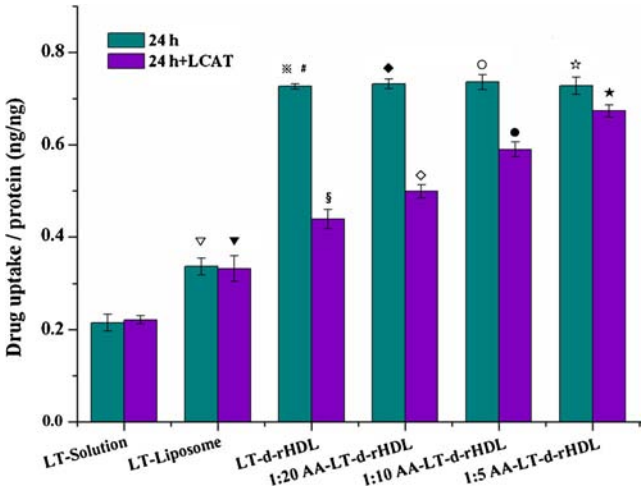

Fig. 10 Cellular drug uptake of different LT preparations by RAW 264.7 with and without LCAT after 24 h culture, among in all intervened-groups concentrations of LT were 20 μM and concentrations of drug carriers (expressed as solid content, μg/mL) including liposome, d-rHDL, 1:20 AA-d-rHDL, 1:10 AA-d-rHDL and 1:5 AA-d-rHDL were 198.1 μg/mL, 208.8 μg/mL, 212.4 μg/mL, 216.2 μg/mL and 223.2 μg/mL, respectively; Significant differences: $\triangledown p<0.05$, LT-L in the absence of LCAT with LT-S in the absence of LCAT, $\blacktriangledown p<0.05$, compared LT-L in the presence of LCAT with LT-S in the presence of LCAT, $\divideontimes p<0.05$, compared LT-d-rHDL with LT-L in the absence of LCAT, $\# p<0.05$, compared LT-d-rHDL in the absence of LCAT with that in the presence of LCAT, $\blacklozenge p<0.05$, compared 1:20 LT-d-rHDL in the absence of LCAT with that in the presence of LCAT, $\circ p<0.05$, compared 1:10 LT-d-rHDL in the absence of LCAT with that in the presence of LCAT, $\star p<0.05$, compared 1:5 LT-d-rHDL in the absence of LCAT with that in the presence of LCAT, $\S p<0.05$, compared LT-d-rHDL in the presence of LCAT with LT-L in the presence of LCAT, $\diamond p<0.05$, compared 1:20 AA-LT-d-rHDL in the presence of LCAT with that LT-d-rHDL in the presence of LCAT, $\bullet p<0.05$, compared 1:10 AA-LT-d-rHDL in the presence of LCAT with 1:20 AA-LT-d-rHDL in the presence of LCAT, $\bigstar p<0.05$, compared 1:5 AA-LT-d-rHDL in the presence of LCAT with 1:10 AA-LT-d-rHDL in the presence of LCAT (mean value ± SD, $n=6$).

that of LT-L ($p<0.05$ for LT-d-rHDL *vs.* LT-L); furthermore, there were no obvious difference between LT-d-rHDL and three AA-LT-d-rHDL preparations.

In the presence of LCAT, there were no significant differences between drug uptake of LT-S with LCAT and that without LCAT, and so did LT-L; however, there were significant differences between drug uptake of LT-d-rHDL with LCAT and without LCAT, and so did three AA-LT-d-rHDL preparations (specifically, $p<0.01$ for of LT-d-rHDL in the absence of LCAT *vs.* LT-d-rHDL in the presence of LCAT, $p<0.05$ for 1:20 AA-LT-d-rHDL in the absence of LCAT *vs.* 1:20 AA-LT-d-rHDL in the presence of LCAT, $p<0.05$ for 1:10 AA-LT-d-rHDL in the absence of LCAT *vs.* 1:10 AA-LT-d-rHDL in the presence of LCAT and $p<0.05$ for 1:5 AA-LT-d-rHDL in the absence of LCAT *vs.* 1:5 AA-LT-d-rHDL in the presence of LCAT, respectively); moreover, with the increment of AA modification amount, the cellular drug uptake was markedly improved in the presence of LCAT (under the action of LCAT, in detail, $p<0.05$ for 1:20 AA-LT-d-rHDL *vs.* LT-d-rHDL, $p<0.05$ for 1:10 AA-LT-d-rHDL *vs.* 1:20 AA-LT-d-rHDL and $p<0.05$ for 1:5 AA-LT-d-rHDL *vs.* 1:10 AA-LT-d-rHDL, respectively).

Inhibition Effects of Different LT Preparations on Macrophage-derived Foam Cell Formation in the Presence of LCAT

Intracellular Lipid Dispositions Stained by Oil Red O

Oil red O staining was performed to visually evaluate the inhibition effects of different LT formulations on macrophage-derived foam cell formation stimulated with oxLDL. It can be seen from Fig. 11 that there was huge lipid deposition stained as red and indicated by positive staining (%) in the positive control group B (76.4±4.2%), compared with normal control group A (3.4±1.5%); moreover, the lipid deposition was increasingly reduced followed as group C (64.5±3.7%), group D (53.3±2.9%), group E (46.6±3.5%), group F (35.1±2.4%), group G (26.6±2.5%) and group H (17.5±3.1%), respectively (specifically, $p<0.01$ for group B *vs.* group A, $p<0.05$ for group C *vs.* group B, $p<0.05$ for group D *vs.* group C, $p<0.05$ for group E *vs.* group D, $p<0.05$ for group F *vs.* group E, $p<0.05$ for group G *vs.* group F and $p<0.05$ for group H *vs.* group G, respectively).

Determination of Intracellular Cholesterol Esters Content

As indicated in the Fig. 12, compared with normal control group A, the CE content (CE content/protein, μg/mg) was extraordinarily increased in the positive control group B ($p<0.01$ for 77.35±3.92 μg/mg of group B *vs.* 8.10±1.28 μg/mg protein of group A); the CE contents were decreased with varying degrees in groups treated with different LT preparations. Specifically, the CE content was reduced in the group C (59.97±2.10 μg/mg) and further reduced followed as group D (48.83±1.71 μg/mg), group E (40.37±2.95 μg/mg), group F (31.42±2.89 μg/mg), group G (26.27±1.25 μg/mg) and group H (21.03±2.40 μg/mg), respectively (specifically, $p<0.01$ for group B *vs.* group A, $p<0.05$ for group C *vs.* group B, $p<0.05$ for group D *vs.* group C, $p<0.05$ for group E *vs.* group D, $p<0.05$ for group F *vs.* group E, $p<0.05$ for group G *vs.* group F and $p<0.05$ for group H *vs.* group G, respectively).

DiI-oxLDL Uptake

As shown in the pictures (Fig. 13) obtained by confocal microscopy and data (Fig. 14) by flow cytometry, the fluorescent signal intensity order in groups from strong to weak were positive control group B (75.48±3.63), group C (63.47±2.94), group D (55.13±4.22), group E (49.92±3.09), group F (43.52±3.52), group G (36.22±4.71), group H (27.63±2.86) and normal control group A (3.99±1.34), respectively

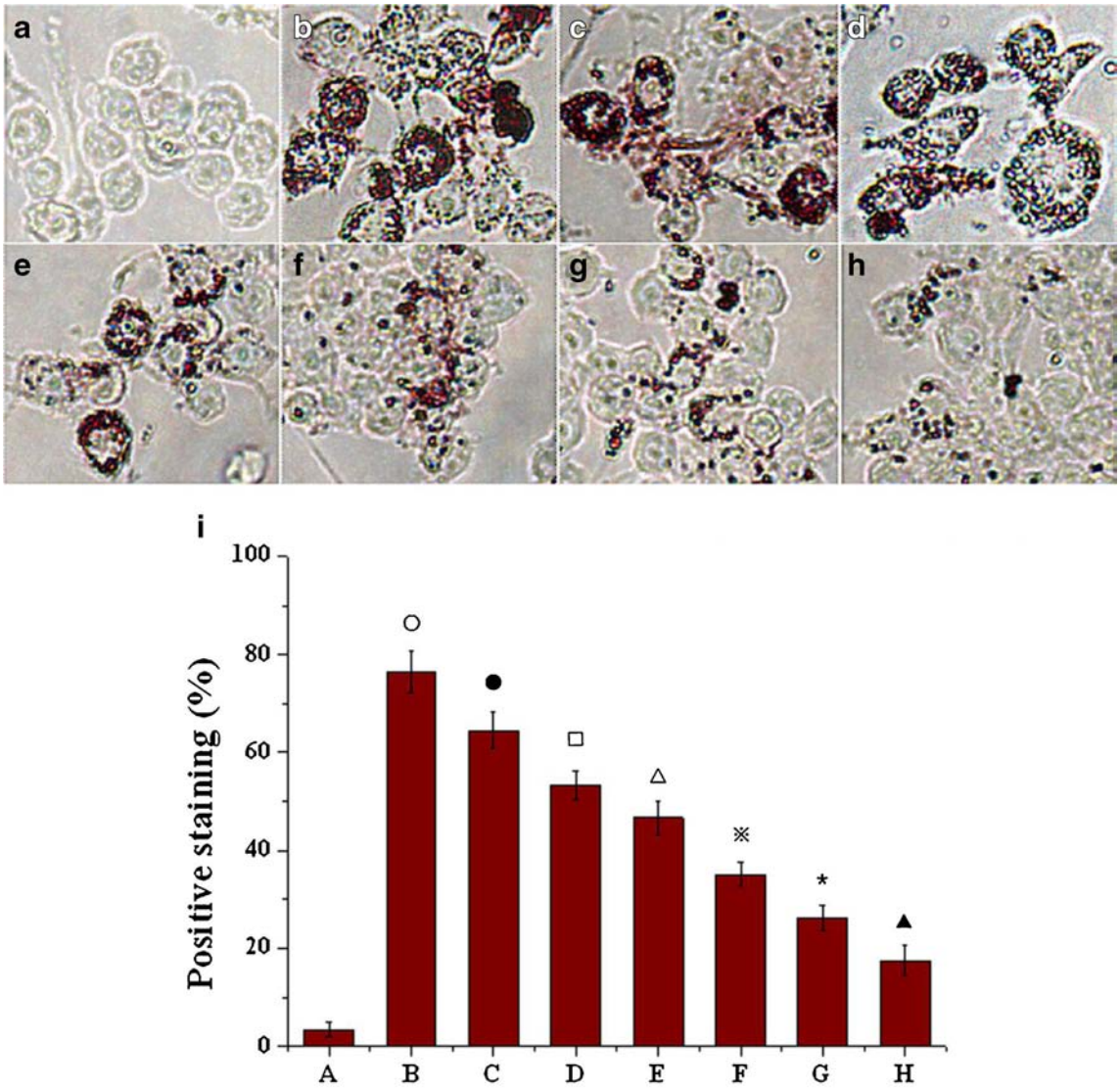

Fig. 11 Intracellular lipid deposition stained by oil red O, among in all intervened-groups concentrations of LT were 20 μM and concentrations of drug carriers (expressed as solid content, μg/mL) including liposome, d-rHDL, 1:20 AA-d-rHDL, 1:10 AA-d-rHDL and 1:5 AA-d-rHDL 198.1 μg/mL, 208.8 μg/mL, 212.4 μg/mL, 216.2 μg/mL and 223.2 μg/mL, respectively; Normal control group (**a**), positive control group (**b**), LT-S (**c**), LT-L (**d**), LT-d-rHDL (**e**), 1:20 AA-LT-d-rHDL (**f**), 1:10 AA-LT-d-rHDL (**g**), 1:5 AA-LT-d-rHDL (**h**) and positive staining analysis (**i**); Significant differences: ○$p<0.01$, compared **b** with **a**, ●$p<0.05$, compared **c** with **b**, □$p<0.05$, compared **d** with **c**, △$p<0.05$, compared **e** with **d**, ※$p<0.05$, compared **f** with **e**, *$p<0.05$, compared **g** with **f**, ☆$p<0.05$, compared **h** with **g** (mean value ± SD, $n=6$).

(specifically, $p<0.01$ for group B *vs.* group A, $p<0.01$ for group C *vs.* group B, $p<0.05$ for group D *vs.* group C, $p<0.05$ for group F *vs.* group E, $p<0.05$ for group G *vs.* group F and $p<0.05$ for group H *vs.* group G, respectively).

RT-PCR and ELISA Assays for IL-6 and TNF-α

In the Fig. 15a and b, mRNA levels (fold change) of both IL-6 and TNF-α were highly enhanced in the positive control group B, compared with normal control group A (towards IL-6, $p<0.01$ for group B *vs.* that of group A; towards TNF-α, $p<0.01$ for group A *vs.* that of group B); moreover, mRNA levels of both IL-6 and TNF-α were decreased in the groups treated with different LT preparation followed as group C, group D, group E, group F, group G and group H, respectively. Specifically, towards IL-6, $p<0.05$ for group C *vs.* group B, $p<0.05$ for group D *vs.* group C, $p<0.05$ for group E *vs.* group D, $p<0.05$ for group F *vs.* group E, $p<0.05$ for group G *vs.* group F and $p<0.05$ for group H *vs.* group E, respectively; towards TNF-α, $p<0.05$ for group C *vs.* group B, $p<0.05$ for group D *vs.* group C, $p<0.05$ for group E *vs.* group D, $p<0.05$ for group F *vs.* group E, $p<0.05$ for group G *vs.* group F and $p<0.05$ for group H *vs.* group G, respectively.

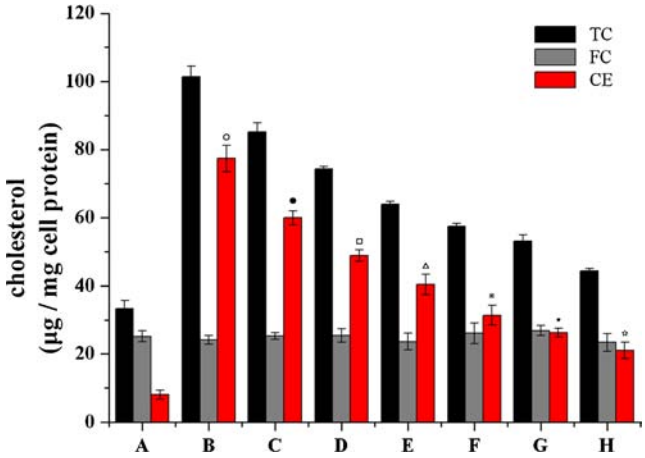

Fig. 12 Determination of intracellular cholesterol esters content, among in all intervened-groups concentrations of LT were 20 μM and concentrations of drug carriers (expressed as solid content, μg/mL) including liposome, d-rHDL, 1:20 AA-d-rHDL, 1:10 AA-d-rHDL and 1:5 AA-d-rHDL were 198.1 μg/mL, 208.8 μg/mL, 212.4 μg/mL, 216.2 μg/mL and 223.2 μg/mL, respectively; Normal control group (**a**), positive control group (**b**), LT-S (**c**), LT-L (**d**), LT-d-rHDL (**e**), 1:20 AA-LT-d-rHDL (**f**), 1:10 AA-LT-d-rHDL (**g**) and 1:5 AA-LT-d-rHDL (**h**); Significant differences: $\circ p < 0.01$, compared **b** with **a**, $\bullet p < 0.05$, compared **c** with **b**, $\square p < 0.05$, compared **d** with **c**, $\triangle p < 0.05$, compared **e** with **d**, $\divideontimes p < 0.05$, compared **f** with **e**, $^{*}p < 0.05$, compared **g** with **f**, $\star p < 0.05$, compared **h** with **g** (mean value ± SD, $n = 6$).

Similar tendencies to mRNA levels of both IL-6 and TNF-α also appeared in the quantitative assay for expressions of both IL-6 and TNF-α, depicted in the Fig. 15c and d. Expressions of both IL-6 and TNF-α (pg/mL) were strikingly boosted in the positive control group B, compared with the normal control group A (towards IL-6, $p<0.01$ for group B *vs.* group A; towards TNF-α, $p<0.01$ for group B *vs.* group A); moreover, expressions of IL-6 and TNF-α were dropped down in groups treated with different LT preparations followed as group C, group D, group E, group F, group G and group H, respectively. In specific, towards IL6, $p<0.05$ for group C *vs.* group B, $p<0.05$ for group D *vs.* group C, $p<0.05$ for group E *vs.* group D, $p<0.05$ for group G *vs.* group F and $p<0.05$ for group H *vs.* group G, respectively; towards TNF-α, $p<0.05$ for group C *vs.* group B, $p<0.05$ for group D *vs.* group C, $p<0.05$ for group E *vs.* group D, $p<0.05$ for group G *vs.* group F and $p<0.05$ for group H *vs.* group G, respectively. However, there were no significant difference between expressions of IL-6 and TNF-α of the groups treated with group F and group E.

RT-PCR and Western Blot Analyses for CD36

As depicted in the Fig. 16a, compared with the normal control group A, mRNA level of CD36 was significantly increased in the positive control group B ($p<0.01$ for group B *vs.* that of group A); moreover, the mRNA levels of CD36 were gradually reduced in the groups treated with different LT preparations followed as group C, group D, group E, group F, group G and group H, respectively (specifically, $p<0.05$ for group C *vs.* group B, $p<0.05$ for group D *vs.* group C, $p<0.05$ for group E *vs.* group D, $p<0.05$ for group F *vs.* group E, $p<0.05$ for group G *vs.* group F and $p<0.05$ for group H *vs.* group G, respectively).

Seen from Fig. 16b, CD36 was remarkably expressed in the positive control group B, compared with positive control group A ($p<0.01$ for group B *vs.* group A); moreover, with intervention of different LT preparations, the similar results to RNA levels of CD36 occurred in the determination of CD36 expression (specifically, $p<0.05$ for group C *vs.* group B, $p<0.05$ for group D *vs.* group C, $p<0.05$ for group E *vs.* group D, $p<0.05$ for group F *vs.* group E, $p<0.05$ for group G *vs.* group F and $p<0.05$ for group H *vs.* group G, respectively). The reduction of CD36 expression by lovastatin administration in our study was consistent with the previous related paper (30,31).

DISCUSSIONS

As one form of native HDL in blood, d-HDL play pivotal functions in the RCT process and have numerous documented functions including anti-thrombotic, anti-inflammatory, anti-oxidant and pro-vasodilatory properties, etc. Moreover, it has been recently demonstrated that d-rHDL loaded with drug had more *in vitro* cellular drug uptake than s-rHDL loaded with drug in the absence of LCAT, probably ascribed to the distinct phospholipids bilayer of d-rHDL similar to the cellular membrane that have better cell fusion property than s-rHDL (5,14). On account of the above-mentioned outstanding biological functions and distinctive discoidal structure embedded by apoAI, d-rHDL had been widely used as drug carriers to improve drug efficacy and reduce side effects. However, our previous research found that drug leaked from d-rHDL loading drug during remodeling behaviors induced by LCAT, thus decreasing drug distribution in target tissues and lowering drug efficacy(5,10,11,14). So how to avoid the undesired drug leakage from d-rHDL loading drug during remodeling behaviors is urgent to be solved.

Hence, our primary purpose of this study was to develop a biomimetic d-rHDL containing drug possessing low reactivity with LCAT, thus efficiently decreasing the undesired drug leakage during remodeling behaviors induced by LCAT in circulation prior to being delivered into target and significantly improving drug efficacy. Among, LT was selected as the model drug, which has been demonstrated strong antiatherogenic efficacies, possibly due to its classical cholesterol-lowering effect, as well as additional pharmacologic activities including antioxidant property, improving the endothelial function, inhibiting platelet aggregation, antithrombotic effect and favoring the stability of vulnerable plaques, etc. (32–35). Moreover, AA was selected as the

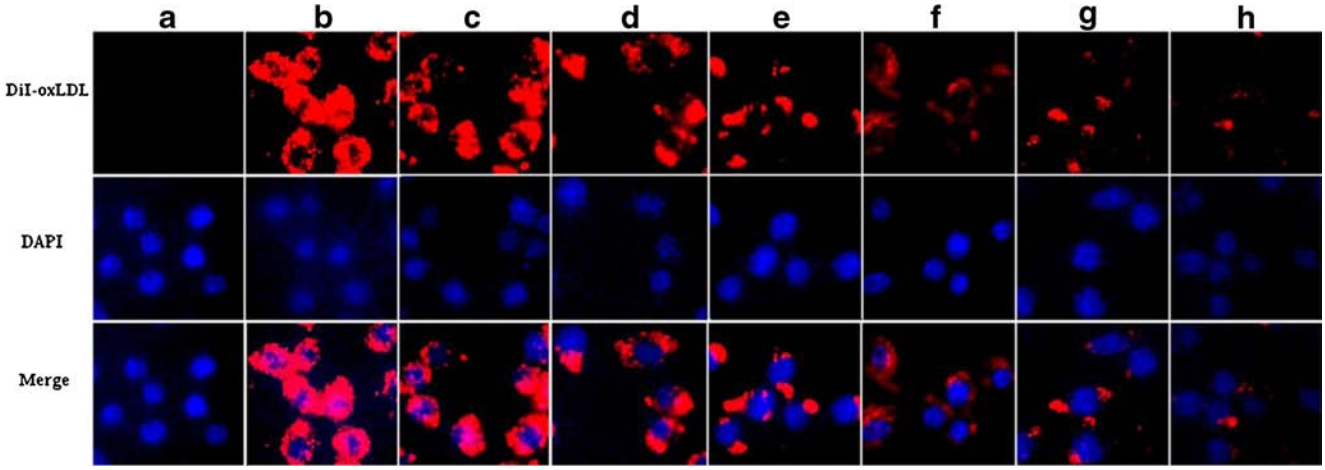

Fig. 13 DiI-oxLDL uptake visualized by confocal microscopy, among in all intervened-groups concentrations of LT were 20 μM and concentrations of drug carriers (expressed as solid content, μg/mL) including liposome, d-rHDL, 1:20 AA-d-rHDL, 1:10 AA-d-rHDL and 1:5 AA-d-rHDL were 198.1 μg/mL, 208.8 μg/mL, 212.4 μg/mL, 216.2 μg/mL and 223.2 μg/mL, respectively; Normal control group (**a**), positive control group (**b**), LT-S (**c**), LT-L (**d**), LT-d-rHDL (**e**), 1:20 AA-LT-d-rHDL (**f**), 1:10 AA-LT-d-rHDL (**g**) and 1:5 AA-LT-d-rHDL (**h**).

modification material to lower the reactivity of LT-d-rHDL with LCAT and reduced the undesired drug leakage, which was mainly based on the following merits of AA: after being inserted into the phospholipids bilayer of d-rHDL, AA would lower the binding extent of apoAI with d-rHDL and enhance the surface negative electricity of d-rHDL, which further had remarkable inhibitory effects on the reactivity of d-rHDL with LCAT similar to those previous related-reports (12,13).

In the present study, AA-LT-d-rHDL preparations with appropriate AA modification amount were first engineered, and then their *in vitro* characterizations were amply investigated and compared. Results from *in vitro* characterizations suggested that as AA increased, AA-LT-d-rHDL had slightly larger diameter and much higher negative surface charge because of electronegative AA incorporation, whereas both EE and DL had not been significantly changed. Among, as the optimized formulations and reconstitution parameters were employed in our current studies, added apoAI could be fully bound with phospholipids bilayer of liposomes to form LT-d-rHDL and three AA-LT-d-rHDL preparations without any free apoAI.

Moreover, binding extent apoAI with LT-d-rHDL verified by GdnHCl denaturation experiments showed that the apoAI in LT-d-rHDL in virtue of the protection of phospholipids bilayer was more resistant to denaturation action of GdnHCl than free apoAI in solution and then had the smallest MDF (seen in the Fig. 3), suggesting that the apoAI in the LT-d-rHDL bound strongly with the phospholipids bilayer of LT-d-rHDL; whereas with the increment of AA modification amount, the MDF of AA-LT-d-rHDL gradually increased and got closer to the MDF of free apoAI in solution. The possible reasons may be as following: AA insertion let phospholipids bilayer of AA-d-rHDL become more fluidity and less packing degree, which were indirectly proved by faster drug release of 1:5 AA-LT-d-rHDL in the absence of LCAT than that of LT-d-rHDL in the absence of LCAT (seen in the Fig. 6). The enhancing fluidity and the reducing packing degree of phospholipids bilayer in AA-LT-d-rHDL increased the fragments poorly binding with AA-LT-d-rHDL in apoAI molecule, and then owing to the lack of protection by phospholipids bilayer, those fragments poorly binding with AA-LT-d-rHDL in apoAI molecule were more susceptible to the denaturation action of GdnHCl than those fragments strongly bound with AA-LT-d-rHDL in apoAI molecule. Hence, all the denaturation processes in Fig. 3 showed two-phase profiles that had fast denaturation of those fragments without protection from phospholipids bilayer in a short while, followed by slow denaturation of those fragments with protection from phospholipids bilayer in the following time. Those two-phase profiles were not totally consistent with the results form Rye *et al.* (15) probably owing to the different modified-materials as well as different pre-determined sample times in those two researches. Collectively, those above results indicated that AA modification raised the surface negative charge of LT-d-rHDL and lowered binding extent of apoAI with LT-d-rHDL.

Furthermore, in the following study, the effects of AA modification on reactivity of LT-d-rHDL with LCAT were investigated through a series of *in vitro* remodeling behaviors evaluation, including changes of physicochemical characteristics such as mean sizes and EE before and after the addition of LCAT, micro-structural transformation visualized by TEM before and after the addition of LCAT, generation of cholesterol esters under LCAT catalysis indicated as reduced cholesterol in preparations and *in vitro* drug release profiles before and after LCAT addition reflecting degree of drug leakage from different preparations. All results from those experiments showed that the reactivity of LT-d-rHDL with LCAT was

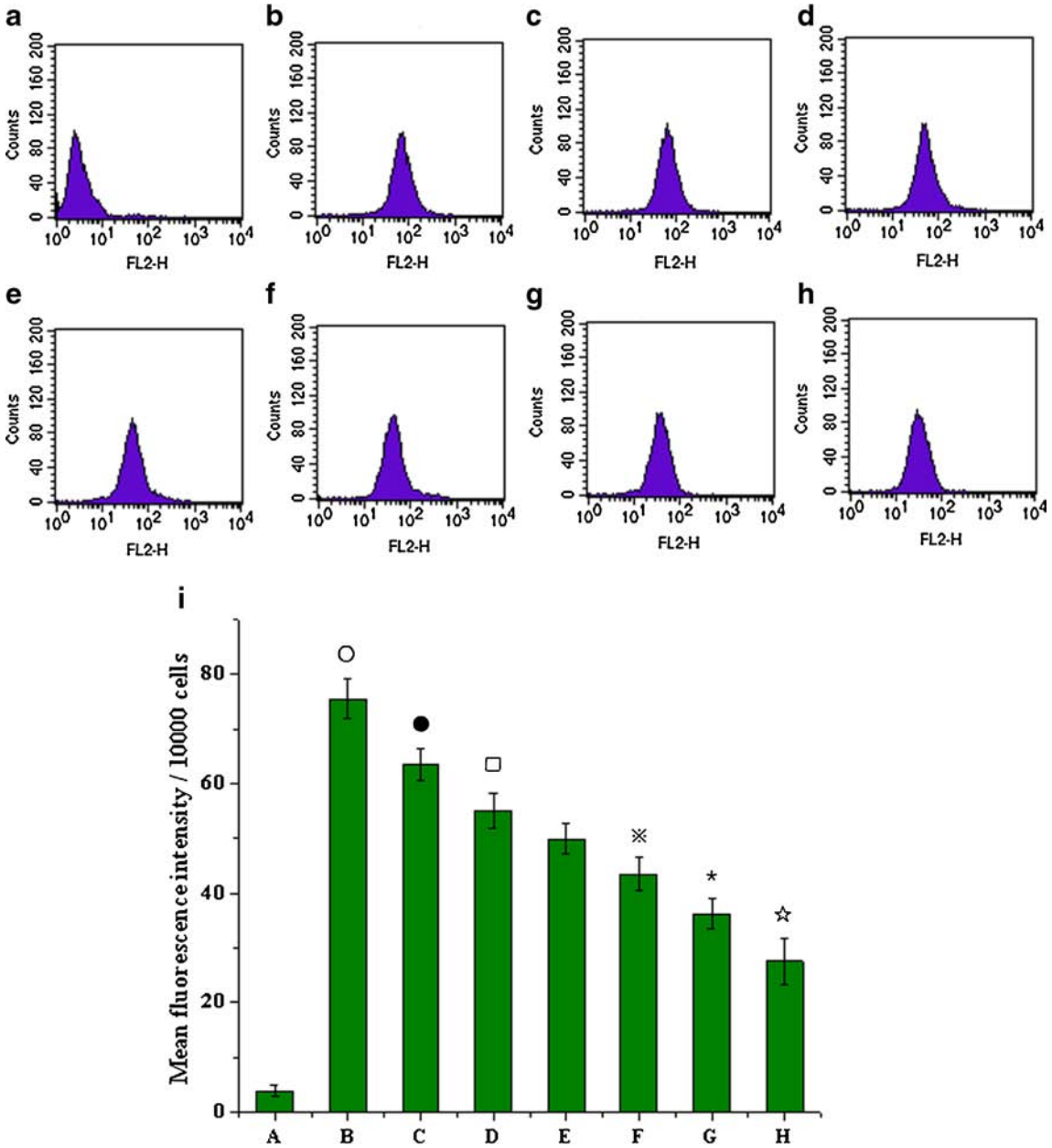

Fig. 14 Mean fluorescent intensity detected by flow cytometry, among in all intervened-groups concentrations of LT were 20 μM and concentrations of drug carriers (expressed as solid content, μg/mL) including liposome, d-rHDL, 1:20 AA-d-rHDL, 1:10 AA-d-rHDL and 1:5 AA-d-rHDL were 198.1 μg/mL, 208.8 μg/mL, 212.4 μg/mL, 216.2 μg/mL and 223.2 μg/mL, respectively; Normal control group (**a**), positive control group (**b**), LT-S (C), LT-L (**d**), LT-d-rHDL (**e**), 1:20 AA-LT-d-rHDL (**f**), 1:10 AA-LT-d-rHDL (**g**), 1:5 AA-LT-d-rHDL (**h**) and positive staining analysis (**i**); Significant differences: ○$p < 0.001$, compared **b** with **a**, ●$p < 0.05$, compared **c** with **b**, □$p < 0.05$, compared **d** with **c**, ※$p < 0.05$, compared **f** with **e**, *$p < 0.05$, compared **g** with **f**, ☆$p < 0.05$, compared **h** with **g** (mean value ± SD, $n = 6$).

increasingly reduced as the AA modification increased, which were characterized by lower mean sizes and higher EE under action of LCAT (Table II), more multi-discoidal fragments in the presence of LCAT visualized by TEM (Fig. 4), fewer *in vitro* generation of cholesterol ester catalyzed by LCAT (Fig. 5) and slower *in vitro* accumulative drug release after 72 h with LCAT as well as more similar *in vitro* release profiles between with LCAT and without LCAT (Fig. 6), respectively. Among them, the 1:5 AA-LT-d-rHDL had the lowest reactivity with LCAT. The reasons for above phenomenon could be explained as follows: on the one hand, after being inserted by AA, the binding extent of apoAI with the phospholipids bilayer of AA-LT-d-rHDL weakened, and further those fragments poorly binding with AA-LT-d-rHDL in apoAI molecule would self-fold and shield the sites for activating the LCAT, which was unfavorable for the reactivity with LCAT (36,37); on the other hand, AA modification increased the surface negative charge of d-rHDL, which repelled the attachment

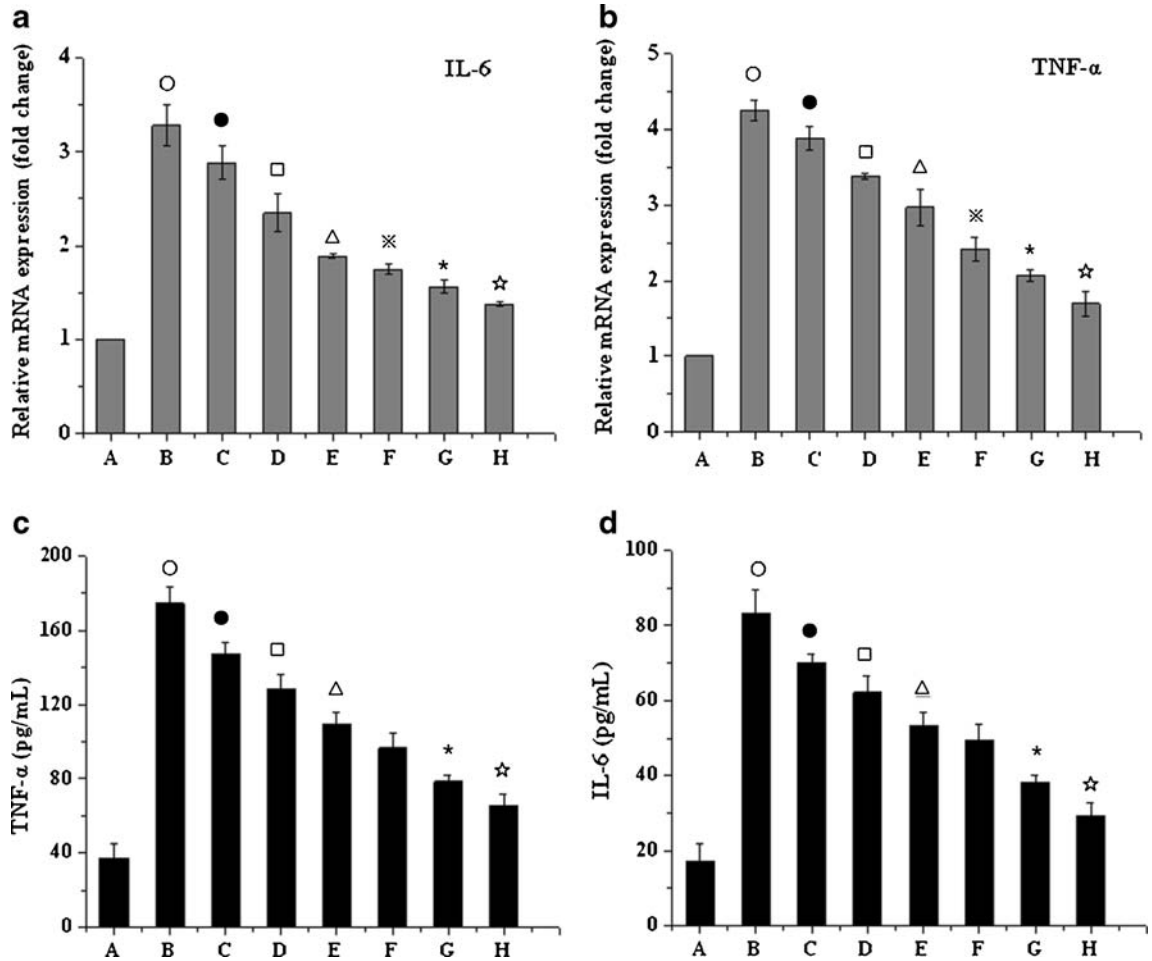

Fig. 15 RT-PCR and ELISA assays for RNA levels of TNF-α and IL-6, among in all intervened-groups concentrations of LT were 20 μM and concentrations of drug carriers (expressed as solid content, μg/mL) including liposome, d-rHDL, 1:20 AA-d-rHDL, 1:10 AA-d-rHDL and 1:5 AA-d-rHDL were 198.1 μg/mL, 208.8 μg/mL, 212.4 μg/mL, 216.2 μg/mL and 223.2 μg/mL, respectively; All in the four figures, normal control group (*A*), positive control group (*B*), LT-S (*C*), LT-L (*D*), LT-d-rHDL (*E*), 1:20 AA-LT-d-rHDL (*F*), 1:10 AA-LT-d-rHDL (*G*), 1:5 AA-LT-d-rHDL (*H*); Significant differences: ○$p < 0.01$, compared *B* with *A*, ●$p < 0.05$, compared *C* with *B*, □$p < 0.05$, compared *D* with *C*, △$p < 0.05$, compared *E* with *D*, ※$p < 0.05$, compared *F* with *E*,*$p < 0.05$, compared *G* with *F*, ☆$p < 0.05$, compared *H* with *G*; (**a**) RT-PCR assay for RNA levels of IL-6, (**b**) RT-PCR assay for RNA levels of IL-6, (**c**) ELISA assays for expressions of IL-6 and (**d**) ELISA assays for expressions of TNF-α (mean value ± SD, $n = 6$).

of AA-LT-d-rHDL to LCAT and thus restrained the reactivity of AA-d-rHDL with LCAT (13,38).

It has been successfully demonstrated that RAW 264.7 can be stimulated with exogenous oxLDL to form foam cell *in vitro* mimicking the important pathologic basis of atherosclerosis (7,25), and 3-hydroxy-3-methyl-glutaryl-CoA reductase (HMG-CoA reductase) activities were too feeble to be detected in RAW 264.7 either cultured in normal conditions or stimulated by exogenous oxLDL in our previous studies (related results not shown here); The main purposes of our current studies were to deliver more lovastatin into cells via d-rHDL as drug carriers and to investigate other anatiatherogenic efficacies of lovastatin (inhibitory effect on the foam cell formation in the macrophage stimulated by exogenous oxLDL) except the classical inhibitory effect on HMG-CoA reductase activity. So RAW 264.7 was chosen as the cell model in the current studies.

In vitro cytotoxicity assays showed that the concentrations of blank drug carriers used in experiments (from nearly 200 μg/mL to 250 μg/mL) nearly had no significant influence on the cell viability. When the concentrations were above 500 μg/mL, slight decrements in cell viability might be caused by excess brought lipids. When the concentrations of blank drug carriers reached 1,500 μg/mL, more obvious cytotoxicities occurred in the three blank AA-d-rHDL preparations, compared with blank liposome and blank d-rHDL (Fig. 7), which probably due to toxic metabolites of the excessive digested AA. Additionally, no significant cytotoxicities were observed in the six LT preparations used in the following cell studies (Fig. 8), which meant that all the six LT preparations we selected in the cell studies were safe and non-toxic.

Experiments on cholesterol efflux (Fig. 9) showed that compared with normal control RAW264.7 cells, LT-d-rHDL and three AA-LT-d-rHDL preparations exhibited no

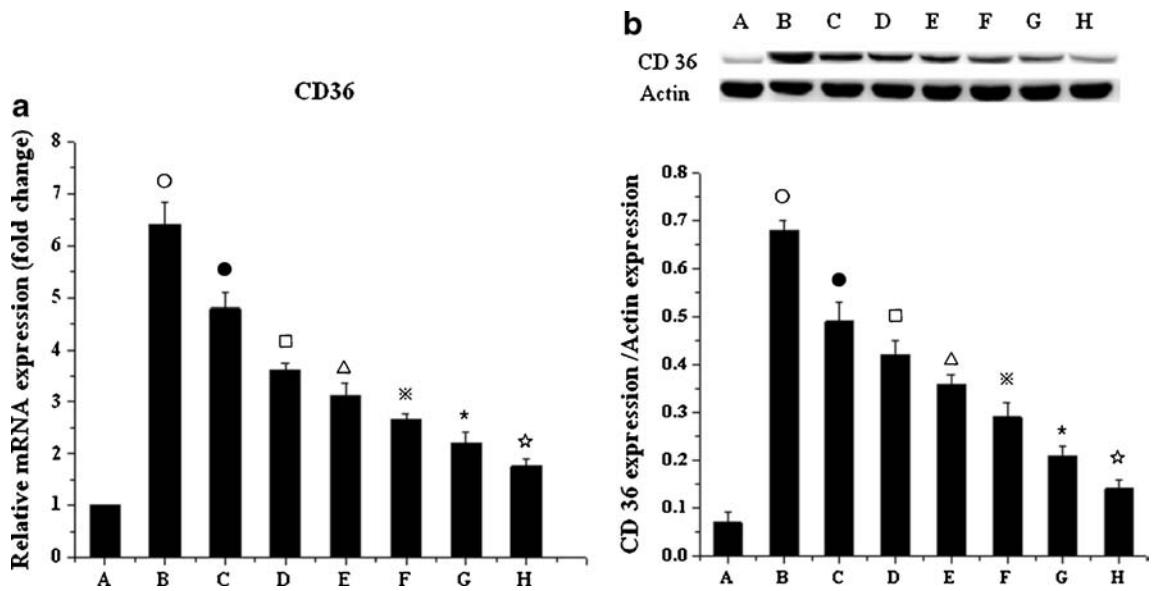

Fig. 16 RT-PCR and western blot analyses for CD36 expression, among in all intervened-groups concentrations of LT were 20 μM and concentrations of drug carriers (expressed as solid content, μg/mL) including liposome, d-rHDL, 1:20 AA-d-rHDL, 1:10 AA-d-rHDL and 1:5 AA-d-rHDL were 198.1 μg/mL, 208.8 μg/mL, 212.4 μg/mL, 216.2 μg/mL and 223.2 μg/mL, respectively; All in the three figures, normal control group (*A*), positive control group (*B*), LT-S (*C*), LT-L (*D*), LT-d-rHDL (*E*), 1:20 AA-LT-d-rHDL (*F*), 1:10 AA-LT-d-rHDL (*G*), 1:5 AA-LT-d-rHDL (*H*) in four figures. Significant differences: ○$p<0.01$, compared *B* with *A*, ●$p<0.05$, compared *C* with *B*, □$p<0.05$, compared *D* with *C*, △$p<0.05$, compared *E* with *D*, ※$p<0.05$, compared *F* with *E*,*$p<0.05$, compared *G* with *F*, ☆$p<0.05$, compared *H* with *G*; (**a**) RT-PCR assay for CD36 and (**b**) Western blot analysis for CD36 (mean value ± SD, $n=6$).

evident cholesterol effluxes from the RAW264.7, which were possibly ascribed to that LT-d-rHDL and three AA-LT-d-rHDL preparations obtained by us had few existing cholesterol used for the stability of the preparations in the reconstitution process, thus lowering the concentration gradient of cholesterol intra and extra-cell for efficient cholesterol efflux. Besides, our previous experiments also showed that the blank drug carriers including liposomes, d-rHDL and three AA-d-rHDL preparations did not exhibit any obvious inhibitory effects on the foam cell formation in RAW 264.7 stimulated with exogenous oxLDL (those related results not shown here). So in the current studies, we paid more attention to the intracellular drug delivery properties of drug carriers including liposomes, d-rHDL and three AA-d-rHDL preparations, ignoring their feeble cholesterol efflux properties.

It has been generally acknowledged that foam cell formation play critical roles in the initiation and progression of atherosclerosis. To be more precise, differentiated from recruited-monocytes from circulation, macrophage in the injured endothelial intima greedily engulf oxLDL by scavenger receptors CD36, then transfer to foam cell, which would secrete amounts of inflammatory cytokines such as tumor necrosis factor-α (TNF-α) and Interleukin-6 (IL-6), etc. and further exacerbate the progression of atherosclerosis. Lipid deposition consisted of massive foam cell are generally referred to as early atherosclerotic lesion. Hence, inhibition of macrophage-derived foam cell formation was generally chosen as an index to evaluate and compare the efficacies of different LT preparation in the current studies (39,40).

In order to further evaluate the effects of AA-LT-d-rHDL on inhibition of macrophage-derived foam cell formation in the presence of LCAT. First, cellular uptakes of different LT preparations with and without LCAT were investigated, respectively, also including the effects of AA modification on the cellular drug uptake of LT-d-rHDL in the presence of LCAT. Related results suggested that in the absence of LCAT, LT-d-rHDL and three AA-LT-d-rHDL preparations markedly improved the cellular drug uptake, compared with LT-S and LT-L; moreover, when in the presence of LCAT, the cellular drug uptake of LT-d-rHDL and three AA-LT-d-rHDL preparations had been significantly reduced, compared with those in the absence of LCAT; however, the AA modification obviously enhanced the cellular drug uptake of LT-d-rHDL in the presence of LCAT (Fig. 10). Specifically, in the presence of LCAT, 1:5 AA-LT-d-rHDL could maintain 92.43 ± 2.65% of cellular drug uptake in the absence of LCAT after 24 h incubation, while 1:10 AA-LT-d-rHDL, 1:20 AA-LT-d-rHDL and LT-d-rHDL only maintained 80.10 ± 3.98%, 68.14 ± 1.12% and 60.41 ± 3.88%, respectively (those data were obtained by the ratio of cellular drug uptake in the presence of LCAT to that in the absence of LCAT).

Furthermore, the efficacies of different LT preparations on inhibition of macrophage-derived foam cell formation in the presence of LCAT were elaborately evaluated and compared by a series of efficacy indexes, such as oil red O staining, intracellular cholesterol esters content, DiI-oxLDL uptake, as well as mRNA levels and expressions of IL-6, TNF-α and CD36, respectively. Results indicated that compared with the

positive control group, the group treated with LT-S showed inferior inhibition effects on macrophage-derived foam cell formation; moreover, LT-L showed slightly stronger efficacy than LT-S; furthermore, obvious inhibition effects on macrophage-derived foam cell formation begun to appear in the groups treated with LT-d-rHDL and three AA-LT-d-rHDL preparations, compared with the other groups; meanwhile, with the increment of AA modification amount, the efficacies were gradually improved and the most potent efficacies occurred in the group treated with 1:5 AA-LT-d-rHDL.

Consequently, all the above outcomes showed that as AA modification amount increased, AA-LT-d-rHDL had lower reactivity with LCAT, less undesired drug leakage during the remodeling behaviors induced by LCAT and more cellular drug uptake, thus exhibiting more potent inhibition effects on macrophage-derived foam cell formation in the presence of LCAT. Especially for 1:5 AA-LT-d-rHDL, 1:5 AA-LT-d-rHDL had the lowest reactivity with LCAT characterized by *in vitro* remodeling behaviors and the most cellular drug uptake owing to the least undesired drug leakage during remodeling behaviors induced by LCAT, thus presenting the most potent efficacies in the presence of LCAT, which were proved by the least intracellular lipid deposition, the lowest intracellular cholesterol esters content, the fewest DiI-oxLDL uptake, and the minimum mRNA levels and expressions of TNF-α, IL-6 and CD36.

Here, our results demonstrated that the intracellular LT amount (Fig. 10) was positively related to the inhibitory effects on the macrophage-derived foam cell formation, which were characterized by lower intracellular lipid deposition (Fig. 11) and less intracellular cholesterol ester accumulation (Fig. 12). Through further investigations, we learned that the possible mechanisms responsible for the inhibitory effects were that the intracellular LT endocytosed via d-rHDL reduced the uptake of oxLDL by RAW 264.7 (Figs. 13 and 14) and then attenuated the inflammatory reaction induced by endocytosed oxLDL in the RAW 264.7 (Fig. 15). Furthermore, through determination of CD 36 expression levels (main receptor for oxLDL), we found that the intracellular LT would suppress the up-regulated expression of CD 36 on RAW 264.7 stimulated with oxLDL (Fig. 16), which could give the explanation to the reduced oxLDL digested by RAW 264.7 with more intracellular LT, thus presenting more potent inhibitory effects on macrophage-derived foam cell formation induced by oxLDL stimulation. All mentioned-above are our supposition mainly based on the related results. In future we will process to verify our induction and might develop other action mechanisms for the inhibitory effects by virtue of other cell lines with or without high HMG-CoA reductase activity, respectively.

CONCLUSIONS

In summary, all the aforementioned results demonstrated that AA modification lowered the reactivity of LT-d-rHDL with LCAT, inhibited the undesired drug leakage during remodeling behaviors induced by LCAT and improved the cellular drug uptake, thus exhibiting potent inhibition on macrophage-derived foam cell formation in the presence of LCAT. Meanwhile, the reactivity of d-rHDL with LCAT could be adjusted by the AA modification amount. Moreover, we process to investigate whether the other polyunsaturated fatty acids such as eicosapentaenoic acid (EPA) and docosahexaenoic acid (DHA) have the similar effects to AA on the reactivity of d-rHDL with LCAT. Furthermore, we will thoroughly investigate the atherosclerotic plaques targeting effects and antiatherogenic efficacies of AA-LT-d-rHDL in atherosclerotic model animals in future. In a word, the ultimate purpose of our studies was to better fulfill targeted-delivery of d-rHDL loaded with drug and provide some notable references for d-rHDL as drug delivery systems.

ACKNOWLEDGMENTS AND DISCLOSURES

This study was financially supported by National Natural Science Foundation of China (No. 81273466), Jiangsu Province Ordinary College and University Innovative Research Programs (No. CXZZ12-0317) and the Special Found Project of Universities' Basic Scientific Research of Central Authorities (No. ZJ11253). We also acknowledged inspiring suggestions from Professor Qi Chen (Department of Pathophysiology, Nan Jing Medical University).

REFERENCES

1. Damiano MG, Mutharasan RK, Tripathy S, McMahon KM, Thaxton CS. Templated high density lipoprotein nanoparticles as potential therapies and for molecular delivery. Adv Drug Deliv Rev. 2012. doi:10.1016/j.addr.2012.07.013.
2. Ding Y, Wang W, Feng M, Wang Y, Zhou J, Ding X, *et al.* A biomimetic nanovector-mediated targeted cholesterol-conjugated siRNA delivery for tumor gene therapy. Biomaterials. 2012;33(34):8893–905.
3. McMahon KM, Mutharasan RK, Tripathy S, Veliceasa D, Bobeica M, Shumaker DK, *et al.* Biomimetic high density lipoprotein nanoparticles for nucleic acid delivery. Nano letters. 2011;11(3):1208–14.
4. Shin J-Y, Yang Y, Heo P, Lee J-C, Kong B, Cho JY, *et al.* pH-responsive high-density lipoprotein-like nanoparticles to release paclitaxel at acidic pH in cancer chemotherapy. Int J Nanomedicine. 2012;7:2805–16.
5. Jia J, Xiao Y, Liu J, Zhang W, He H, Chen L, *et al.* Preparation, characterizations, and in vitro metabolic processes of paclitaxel-loaded discoidal recombinant high-density lipoproteins. Journal of pharmaceutical sciences. 2012;101(8):2900–8.
6. Zhang W, He H, Liu J, Wang J, Zhang S, Zhang S, *et al.* Pharmacokinetics and atherosclerotic lesions targeting effects of

tanshinone IIA discoidal and spherical biomimetic high density lipoproteins. Biomaterials. 2012;34(1):306–19.
7. Gu X, Zhang W, Liu J, Shaw JP, Shen Y, Xu Y, *et al.* Preparation and characterization of a lovastatin-loaded protein-free nanostructured lipid carrier resembling high-density lipoprotein and evaluation of its targeting to foam cells. AAPS PharmSciTech. 2011;12(4):1200–8.
8. Brewer Jr HB. High-Density Lipoprotein Metabolism. Atlas of Atherosclerosis and Metabolic Syndrome: Springer; 2011. p. 93–111.
9. Sviridov D. High-density lipoproteins: structure, metabolism, function and TherapeuticsBy anatol kontush and M. John Chapman. Chem Med Chem. 2013;8(4):669–70.
10. Wang J, Jia J, Liu J, He H, Zhang W, Li Z. Tumor targeting effects of a novel modified paclitaxel-loaded discoidal mimic high density lipoproteins. Drug Delivery. 2013;0:1–8.
11. Zhang M, Jia J, Liu J, He H, Liu L. A novel modified paclitaxel-loaded discoidal recombinant high-density lipoproteins: preparation, characterizations and in vivo evaluation. Asian Journal of Pharmaceutical Sciences. 2013.
12. Huggins KW, Curtiss LK, Gebre AK, Parks JS. Effect of long chain polyunsaturated fatty acids in the sn-2 position of phosphatidylcholine on the interaction with recombinant high density lipoprotein apolipoprotein AI. Journal of lipid research. 1998;39(12):2423–31.
13. Sparks DL, Chatterjee C, Young E, Renwick J, Pandey NR. Lipoprotein charge and vascular lipid metabolism. Chemistry and physics of lipids. 2008;154(1):1–6.
14. Zhang W-L, Xiao Y, Liu J-P, Wu Z-M, Gu X, Xu Y-M, *et al.* Structure and remodeling behavior of drug-loaded high density lipoproteins and their atherosclerotic plaque targeting mechanism in foam cell model. International journal of pharmaceutics. 2011;419(1):314–21.
15. Rye K-A, Hime NJ, Barter PJ. The influence of sphingomyelin on the structure and function of reconstituted high density lipoproteins. J Biol Chem. 1996;271(8):4243–50.
16. Kontogiannopoulos KN, Assimopoulou AN, Dimas K, Papageorgiou VP. Shikonin-loaded liposomes as a new drug delivery system: physicochemical characterization and in vitro cytotoxicity. Eur J Lipid Sci Technol. 2011;113(9):1113–23.
17. Su Z, Niu J, Xiao Y, Ping Q, Sun M, Huang A, *et al.* Effect of octreotide–polyethylene glycol (100) monostearate modification on the pharmacokinetics and cellular uptake of nanostructured lipid carrier loaded with hydroxycamptothecine. Molecular pharmaceutics. 2011;8(5):1641–51.
18. Yang L, Ling W, Ma J, Tang Z, Wu C. Effect of lysophosphatidylcholine on cholesterol efflux from macrophage foam cells. Chinese Journal of Pathophysiology. 2002;18(1):28–31.
19. Murakami T, Wijagkanalan W, Hashida M, Tsuchida K. Intracellular drug delivery by genetically engineered high-density lipoprotein nanoparticles. Nanomedicine. 2010;5(6):867–79.
20. Hofnagel O, Luechtenborg B, Weissen-Plenz G, Robenek H. Statins and foam cell formation: impact on LDL oxidation and uptake of oxidized lipoproteins via scavenger receptors. Biochimica et biophysica acta (BBA)-molecular and cell biology of. Lipids. 2007;1771(9):1117–24.
21. Lin J, Li M, Wang Z, He S, Ma X, Li D. The role of CD4+ CD25+ regulatory T cells in macrophage-derived foam-cell formation. Journal of lipid research. 2010;51(5):1208–17.
22. Xu G, Watanabe T, Iso Y, Koba S, Sakai T, Nagashima M, *et al.* Preventive effects of heregulin-β1 on macrophage foam cell formation and atherosclerosis. Circulation research. 2009;105(5):500–10.
23. Zhao Z-Z, Wang Z, Li G-H, Wang R, Tan J-M, Cao X, *et al.* Hydrogen sulfide inhibits macrophage-derived foam cell formation. Experimental Biology and Medicine. 2011;236(2):169–76.
24. Liu G, Ma S, Li S, Cheng R, Meng F, Liu H, *et al.* The highly efficient delivery of exogenous proteins into cells mediated by biodegradable chimaeric polymersomes. Biomaterials. 2010;31(29):7575–85.
25. Xu S, Liu Z, Huang Y, Le K, Tang F, Huang H, *et al.* Tanshinone IIa inhibits oxidized LDL-induced LOX-1 expression in macrophages by reducing intracellular superoxide radical generation and NF-κB activation. Transl Res. 2012;160(2):114–24.
26. Sung HJ, Kim J, Kim Y, Jang S-W, Ko J. N-acetyl cysteine suppresses the foam cell formation that is induced by oxidized low density lipoprotein via regulation of gene expression. Molecular biology reports. 2012;39(3):3001–7.
27. Hata H, Sakaguchi N, Yoshitomi H, Iwakura Y, Sekikawa K, Azuma Y, *et al.* Distinct contribution of IL-6, TNF-α, IL-1, and IL-10 to T cell–mediated spontaneous autoimmune arthritis in mice. J Clin Investig. 2004;114(4):582–8.
28. Ishii T, Itoh K, Ruiz E, Leake DS, Unoki H, Yamamoto M, *et al.* Role of nrf2 in the regulation of cd36 and stress protein expression in murine macrophages activation by oxidatively modified LDL and 4-hydroxynonenal. Circulation research. 2004;94(5):609–16.
29. Xie C, Kang J, Chen J-R, Lazarenko OP, Ferguson ME, Badger TM, *et al.* Lowbush blueberries inhibit scavenger receptors CD36 and SR-a expression and attenuate foam cell formation in ApoE-deficient mice. Food & Function. 2011;2(10):588–94.
30. Hrboticky N, Draude G, Hapfelmeier G, Lorenz R, Weber P. Lovastatin decreases the receptor-mediated degradation of acetylated and oxidized LDLs in human blood monocytes during the early stage of differentiation into macrophages. Arteriosclerosis, thrombosis, and vascular biology. 1999;19(5):1267–75.
31. Pietsch A, Erl W, Lorenz RL. Lovastatin reduces expression of the combined adhesion and scavenger receptor CD36 in human monocytic cells. Biochemical pharmacology. 1996;52(3):433–9.
32. Lin R, Liu J, Peng N, Yang G, Gan W, Wang W. Lovastatin reduces nuclear factor κB activation induced by C-reactive protein in human vascular endothelial cells. Biol Pharm Bull. 2005;28(9):1630–4.
33. Miyata R, Hiraiwa K, Cheng JC, Bai N, Vincent R, Francis GA, *et al.* Statins attenuate the development of atherosclerosis and endothelial dysfunction induced by exposure to urban particulate matter (PM_{10}). Pharmacology: Toxicology and Applied; 2013.
34. Obi C, Wysokinski W, Karnicki K, Owen WG, McBane RD. Inhibition of platelet-rich arterial thrombus in vivo acute antithrombotic effect of intravenous HMG-CoA Reductase therapy. Arteriosclerosis, thrombosis, and vascular biology. 2009;29(9):1271–6.
35. Koh KK. Effects of statins on vascular wall: vasomotor function, inflammation, and plaque stability. Cardiovascular research. 2000;47(4):648–57.
36. Parks JS, Huggins KW, Gebre AK, Burleson ER. Phosphatidylcholine fluidity and structure affect lecithin: cholesterol acyltransferase activity. Journal of lipid research. 2000;41(4):546–53.
37. Rye K-A, Duong M, Psaltis MK, Curtiss LK, Bonnet DJ, Stocker R, *et al.* Evidence that phospholipids play a key role in pre-β apoA-I formation and high-density lipoprotein remodeling. Biochemistry. 2002;41(41):12538–45.
38. Stamler CJ, Breznan D, Neville TA, Viau FJ, Camlioglu E, Sparks DL. Phosphatidylinositol promotes cholesterol transport in vivo. Journal of lipid research. 2000;41(8):1214–21.
39. Tian L, Luo N, Zhu X, Chung B-H, Garvey WT, Fu Y. Adiponectin-AdipoR1/2-APPL1 signaling axis suppresses human foam cell formation: differential ability of AdipoR1 and AdipoR2 to regulate inflammatory cytokine responses. Atherosclerosis. 2012;221(1):66–75.
40. Libby P, Okamoto Y, Rocha VZ, Folco E. Inflammation in atherosclerosis. Circ J. 2010;74:213–20.